AD-781 280

MAZE 3 - A SEQUENTIAL COMPUTER SPECTRAL ENHANCEMENT CODE: STUDIED FOR CONVERSION TO ILLIAC IV

Louis Huszar, et al

Science Applications, Incorporated

Prepared for:

Defense Nuclear Agency
Defense Advanced Research Projects Agency

December 1973

DISTRIBUTED BY:

NTIS

National Technical Information Service
U. S. DEPARTMENT OF COMMERCE
5285 Port Royal Road, Springfield Va. 22151

UNCLASSIFIED

SECURITY CLASSIFICATION OF THIS PAGE (When Data Entered)

AD-781280

REPORT DOCUMENTATION PAGE		READ INSTRUCTIONS BEFORE COMPLETING FORM
1. REPORT NUMBER DNA 3274F	2. GOVT ACCESSION NO.	3. RECIPIENT'S CATALOG NUMBER
4. TITLE (and Subtitle) MAZE3 - A SEQUENTIAL COMPUTER SPECTRAL ENHANCEMENT CODE, Studied for Conversion to ILLIAC IV		5. TYPE OF REPORT & PERIOD COVERED Final Report 1 Nov 72 - 31 Jan 74
		6. PERFORMING ORG. REPORT NUMBER SAI-73-649-LJ
7. AUTHOR(s) Louis Huszar, John H. Reed, Martin Sperling		8. CONTRACT OR GRANT NUMBER(s) DNA001-73-C-0026
9. PERFORMING ORGANIZATION NAME AND ADDRESS Science Applications, Inc. 1200 Prospect Street La Jolla, California 92037		10. PROGRAM ELEMENT, PROJECT, TASK AREA & WORK UNIT NUMBERS DARPA Order No. 2247 RMSS Code M99QAHPE074 Work Unit No. 01
11. CONTROLLING OFFICE NAME AND ADDRESS Director Defense Nuclear Agency Washington, D.C. 20305		12. REPORT DATE December 1973 13. NUMBER OF PAGES 74
14. MONITORING AGENCY NAME & ADDRESS (if different from Controlling Office) Director Defense Advanced Research Projects Agency Arlington, Virginia 22209		15. SECURITY CLASS. (of this report) Unclassified 15a. DECLASSIFICATION DOWNGRADING SCHEDULE

16. DISTRIBUTION STATEMENT (of this Report)

Approved for public release; distribution unlimited.

17. DISTRIBUTION STATEMENT (of the abstract entered in Block 20, if different from Report)

18. SUPPLEMENTARY NOTES

19. KEY WORDS (Continue on reverse side if necessary and identify by block number)

Spectral unfolding
Spectral enhancement

Reproduced by
NATIONAL TECHNICAL
INFORMATION SERVICE
U.S. Department of Commerce
Springfield VA 22151

20. ABSTRACT (Continue on reverse side if necessary and identify by block number)

A mathematical model is described which forms the basis of a spectral enhancement program that follows along the lines of the MAZE series of spectral unfolding codes. The treatment of a priori and a posteriori information functions are elaborated as well as their optimization and subsequent implementation. The code was developed for a serial computer and the results are demonstrated for several examples. The code has also been converted to the Illiac IV parallel processor computer system in the Glypnir language.

DD FORM 1 JAN 73 1473 EDITION OF 1 NOV 65 IS OBSOLETE

UNCLASSIFIED

SECURITY CLASSIFICATION OF THIS PAGE (When Data Entered)

SUMMARY

A mathematical model is described which forms the basis of a spectral enhancement program that follows along the lines of the MAZE series of spectral unfolding codes. The treatment of a priori and a posteriori information functions are elaborated as well as their optimization and subsequent implementation. The code was developed for a serial computer and the results are demonstrated for several examples. The code has also been converted to the Illiac IV parallel processor computer system in the Glypnir language.

CONTENTS

Section		Page
1.	INTRODUCTION	7
2.	PRINCIPLES OF UNFOLDING	9
3.	OPTIMIZATION CRITERIA	25
	3.1 A Posteriori Information	27
	3.2 A Priori Information	33
	3.3 Transformation to Equivalent Counts	38
4.	IMPLEMENTATION OF THE OPTIMIZATION	41
5.	RESPONSE FUNCTION PARAMETERIZATION	51
6.	EXAMPLES OF SPECTRAL ENHANCEMENT	57
	6.1 Example 1, Simulated Data	57
	6.2 Example 2, Simulated Data	65
	6.3 Example 3, Si(Li) X-ray Data	67
	6.4 Example 4, Ge(Li) Gamma-ray Data	69
7.	CONCLUSION	77
REFERENCES		79
DISTRIBUTION LIST		81

LIST OF ILLUSTRATIONS

		Page
1.	Ge(Li) line shape at 2 MeV	53
2.	Simulated x-ray data	59
3.	Image spectrum (enhanced spectrum)	60
4.	Deviations	62
5.	Discrete spectrum	63
6.	Continuum	64
7.	Simulated x-ray data	66
8.	Image spectrum (enhanced spectrum)	68
9.	X-ray fluorescence data	70
10.	Enhanced x-ray fluorescence spectrum	71
11.	Ge(Li) gamma-ray data	72
12.	Enhanced gamma-ray spectrum	74
13.	Improved enhanced gamma-ray spectrum	75

1. INTRODUCTION

The MAZE series of computer programs are general purpose estimation codes that are and have been used for unfolding, resolution enhancement, smoothing, interpolation and fitting. MAZE1[1] and MAZE2[2] have been sponsored by the Defense Nuclear Agency. This report describes the development of an improved version of MAZE2, now designated MAZE3 and the subsequent conversion of this improved version of Illiac IV (I4) which is designated MAZE4. It should be emphasized that this effort was not strictly a conversion of an existing computer program from a serial computer to the I4 computer. Rather, there was a great deal of emphasis placed on introducing the latest information theory techniques into MAZE3 and debugging a code that would work very well for serial computers. Only after this was accomplished was the code then fitted to the I4 computer to take advantage of the unique computational advantages provided by that system.

The I4 is a parallel computer system basically consisting of a Control Unit (CU) and 64 Processing Elements (PE's). The PE's work in parallel and can execute 64 instructions simultaneously. The CU can also be executing instructions at the same time. The obvious advantage of the I4 over serial computers is the simultaneous execution of up to 64 instructions; however, they have to be the same instruction. In each PE the instructions operate on data elements within the individual PE's own memory.

Surrounding the I4 system is a great deal of peripheral storage which will be useful when MAZE is being used for unfolding a spectrum with a large number of channels. It is possible (although perhaps not very practical, as will be described later) to parameterize the response data from Ge(Li) detectors in order to minimize the size of the response matrix. However, the manner in which MAZE is expected to be used on I4 is that the full response matrix will be necessary. Thus, the use of the peripheral storage (I4 disk) is imperative. Also, since the computation time goes up as the square of the increased number of channels, it is evident that the I4 system can be an effective tool for unfolding.

Section 2 describes the principles of unfolding which form the basis of the mathematical model. Section 3 elaborates upon a specific form of the optimization function and Section 4 explains the method of implementation. Section 5 has some comments on the parameterization of the Ge(Li) response function, while Section 6 contains some specific examples of unfolding.

2. PRINCIPLES OF UNFOLDING

The underlying mathematical principles of unfolding are well covered elsewhere, [1,2] nonetheless parts of it will be reproduced here for completeness.

The system consisting of source, spectrometer, unfolding processor, and receiver involves the following flow of information:

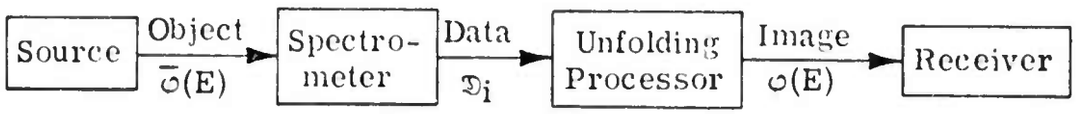

The object spectrum $\bar{\sigma}(E)$, is the energy distribution of neutrons or gammas from the source. It is viewed by the spectrometer, which produces a data vector, $\mathfrak{D}_i$. $\mathfrak{D}$ has passed through a complex detection process and suffers from loss of resolution, from particle recoil effects, and from noise due to statistical fluctuations of the discrete count data. It is the job of the unfolding processor to minimize the effects of the spectrometer response and the count fluctuations, and to construct from the data an image spectrum, $\sigma(E)$, that corresponds closely to the true object, transmitting this image spectrum to the receiver.

One way of viewing the unfolding processor is in terms of its objective. How closely the image function, σ, corresponds to the object function, $\bar{\sigma}$, is a measure of the effectiveness of the unfolding

processor. Generally there is a distance function, $s(\varphi, \bar{\varphi})$, which tells how far a given φ is separated from a given $\bar{\varphi}$. Given the true object $\bar{\varphi}$, the optimum image, φ, is the one for which $s(\varphi, \bar{\varphi})$ is as small as possible. This is of conceptual interest but of no practical utility, because if $\bar{\varphi}$ were known there would be no need for a measurement. However, one can construct a function W which measures the effectiveness of the unfolding processor, but which is a function only of quantities that are input to or output from the processor, that is

$$W = W(\mathfrak{D}, \varphi) \quad .$$

Then, given the data set, $\mathfrak{D}$, the optimum image would be the one for which $W(\mathfrak{D}, \varphi)$ is as small as possible.

Let us begin with a more precise statement of the optimization principle: There is a function of the data $\mathfrak{D}$ and the image estimate φ,

$$W(\mathfrak{D}, \varphi) \quad ,$$

such that for a given data set the optimum image under the W-criterion occurs at that φ which minimizes W. The principle does not say that the resulting φ is universally optimum, only optimum under the criterion defined by W. It remains for the inventors of W-functions to insure that they have a precise understanding of what constitutes an optimum image and that they are accurately translating that understanding into mathematical forms.

The next important point is that W can be thought of as an information function. Information functions are related to probability

distributions in a simple, precisely defined way, and we now explain that relationship.

Information has to do with reduction of the unknown, that is with the specification of quantities that had been random relative to previously acquired knowledge. The shape and magnitude of an energy spectrum are such quantities. Before actual measurement no definite statement can be made. At best a probability density can be assigned to a given shape and magnitude, based upon known characteristics of the source and known distributions among populations of sources. Certain classes of conceivable configurations may be ruled out as occurring with vanishingly small probability, and this fact will be used in the unfolding process; but the idea that a given spectrum is, even before measurement, of definite shape and magnitude is of no practical utility when these parameters are unknown.

If a measurement could determine these parameters, an amount of information would be acquired. The amount would depend upon the rarity of the spectrum that was observed. That observation of a common spectral shape conveys a smaller amount of information than observation of a rare spectral shape agrees with the intuitive notion of information, as does the idea that the observation of two spectra with similar shapes conveys twice as much information as observation of one. Suppose the probability of that shape is p; then the probability of n spectra with that shape is $P = p^n$. Consequently, the desired additivity of information is guaranteed if it has the form

$$W = k \ell n P \quad ,$$

where k is a constant and ℓn stands for the natural logarithm, since it is a property of logarithms that

$$\ell n\, p^n = n \ell n P \quad .$$

There is no particular significance to the value of k or to the choice of logarithmic base other than to define units of information. It is customary to take

$$W = -\ell n P \quad .$$

The minus sign is necessary because information increases as probability decreases.

Now, a generalization of the simple probability p, is the probability distribution $f(\overline{\varphi})$. If we imagine a space of all possible spectra $\overline{\varphi}$ such that each $\overline{\varphi}$ is a point in the space, and if $d\Omega$ is an infinitesimal volume surrounding such a point, then

$$dp = f(\overline{\varphi})\, d\Omega$$

is the infinitesimal probability of finding $\overline{\varphi}$ in $d\Omega$. That is a definition. We can turn it around, write

$$f(\overline{\varphi}) = \frac{dp}{d\Omega} \quad ,$$

and think of $f(\overline{\varphi})$ as the density of probability at $\overline{\varphi}$. The corresponding generalization of information is the information function

$$W = -\ell n\, f \quad .$$

As before, information is additive when probability is multiplicative. Notice a very important property of the information function that the point of minimum information corresponds to the point of maximum probability.

The information function required for unfolding is complex conceptually, because it involves two random states, the data and the image. Let us next consider this complication, first from the viewpoint of probabilistic arguments that motivate it, and secondly from the viewpoint of intuitive notions of why it works. The coordinate (E) and the analogous subscript (i) are unimportant to this discussion, and will be dropped. What is most important, is the fact that object, data, and image are random variables.

We have already considered the fact that before measurement the object function is random relative to available knowledge. We called its probability distribution, $f(\overline{\varphi})$. After measurement $\overline{\varphi}$ is not reduced to certainty. It is still a random variable, but its probability distribution $f(\overline{\varphi}|\mathfrak{D})$ is reduced in size. We have not discussed the size of probability distributions and will not, but the precise notion defined in terms of entropy corresponds to the intuitive notion that a probability distribution is smaller or tighter when the range of probable variation is decreased. In the distribution $f(\overline{\varphi}|\mathfrak{D})$, known as the "conditional probability of $\overline{\varphi}$-if-$\mathfrak{D}$", $\overline{\varphi}$ is thought of as a random variable, and $\mathfrak{D}$ is thought of as fixed.

Of course it is also possible to think of the data $\mathfrak{D}$ as random. If a measurement of a known state $\bar{\sigma}$ is made, say of a test source, the data that would result from an ensemble of separate measurements with the gamma camera would be distributed probabilistically with some distribution $f(\mathfrak{D}|\bar{\sigma})$, primarily due to the discrete nature of the gamma flux. This time $\mathfrak{D}$ is thought of as the random variable and $\bar{\varphi}$ is thought of as fixed, and the resulting probability distribution $f(\mathfrak{D}|\bar{\sigma})$ is called the conditional probability of $\mathfrak{D}$-if-$\bar{\sigma}$. It is important to realize that $f(\mathfrak{D}|\bar{\sigma})$ contains a mathematical model of the camera response as well as of the fluctuation process, since both are necessary for defining the distribution of $\mathfrak{D}$. It is also worth remarking that so far the symbol f has been used to specify three different distributions, $f(\bar{\sigma})$, $f(\bar{\varphi}|\mathfrak{D})$, and $f(\mathfrak{D}|\bar{\sigma})$, with the hope that the different argument structures will be sufficient to distinguish them. The freest possible variation of $\mathfrak{D}$ occurs when $\bar{\varphi}$ is unspecified. The associated distribution, which of course is larger than $f(\mathfrak{D}|\bar{\sigma})$, we call $f(\mathfrak{D})$.

One more distribution involving $\bar{\varphi}$ and $\mathfrak{D}$: if nothing is known, neither the state of the source nor the state of the data, then both must be treated as random. A product space may be formed such that each point in space corresponds to a pair $(\bar{\sigma}, \mathfrak{D})$. The associated probability density $f(\bar{\varphi}, \mathfrak{D})$ is known as the joint probability of $\bar{\varphi}$ and $\mathfrak{D}$.

Now this distribution, the joint distribution of $\bar{\sigma}$ and $\mathfrak{D}$, is a complete specification of the random properties of $\bar{\sigma}$ and $\mathfrak{D}$, and

therefore determines the four previous distributions. The distribution of $\overline{\varphi}$ is just the joint distribution of $\overline{\varphi}$ and $\mathfrak{D}$ with integration over all possible $\mathfrak{D}$:

$$f(\overline{\varphi}) = \int_{\text{all } \mathfrak{D}} \cdots \int f(\overline{\varphi}, \mathfrak{D})\ d\Omega_{\mathfrak{D}} \quad .$$

The distribution of $\mathfrak{D}$ is the joint distribution of $\overline{\varphi}$ and $\mathfrak{D}$ with integration over all possible $\overline{\varphi}$:

$$f(\mathfrak{D}) = \int_{\overline{\varphi}} \cdots \int f(\overline{\varphi}, \mathfrak{D})\ d\Omega_{\overline{\varphi}} \quad .$$

The relationship with the conditional probability of $\overline{\varphi}$-if-$\mathfrak{D}$ is

$$f(\overline{\varphi}, \mathfrak{D}) = f(\overline{\varphi} \mid \mathfrak{D})\ f(\mathfrak{D}) \quad ,$$

because the probability of $\mathfrak{D}$ being an infinitesimal volume $d\Omega_{\mathfrak{D}}$ about $\mathfrak{D}$ is

$$f(\mathfrak{D})\ d\Omega_{\mathfrak{D}} \quad ,$$

while the probability of $\overline{\varphi}$ being simultaneously in $d\Omega_{\overline{\varphi}}$ about $\overline{\varphi}$ is

$$f(\overline{\varphi} \mid \mathfrak{D})\ d\Omega_{\overline{\varphi}} \quad ,$$

the compound probability being

$$f(\overline{\varphi}, \mathfrak{D})\ d\Omega_{\overline{\varphi}}\ d\Omega_{\mathfrak{D}} = f(\overline{\varphi} \mid \mathfrak{D})\ d\Omega_{\overline{\varphi}}\ f(\mathfrak{D})\ d\Omega_{\mathfrak{D}} \quad .$$

By the same token, the relationship with the conditional probability of $\mathfrak{D}$-if-$\overline{\varphi}$ is

$$f(\overline{\varphi}, \mathfrak{D}) = f(\mathfrak{D} \mid \overline{\varphi})\ f(\overline{\varphi}) \quad .$$

Finally, the fact that the two conditional probabilities are related to the joint probability means that they are themselves related by the very important equation

$$f(\overline{\varphi} \mid \mathfrak{D})\ f(\mathfrak{D}) = f(\mathfrak{D} \mid \overline{\varphi})\ f(\overline{\varphi}) \quad .$$

This implies that any one of the conditional or single probabilities can be expressed in terms of the other three.

All the probability distributions have an analogous information function defined by the logarithmic relationship

$$W = - \ln f$$

mentioned previously. Here they are: The information function of $\overline{\varphi}$, $W(\varphi)$; and the information function of $\mathfrak{D}$, $W(\mathfrak{D})$. The conditional information function of $\overline{\varphi}$-if-$\mathfrak{D}$, $W(\overline{\varphi} \mid \mathfrak{D})$; and the conditional information function of $\mathfrak{D}$-if-$\overline{\varphi}$, $W(\mathfrak{D} \mid \overline{\varphi})$. The joint information function of $\overline{\varphi}$ and $\mathfrak{D}$, $W(\varphi, \mathfrak{D})$. Again we mention that the same symbol, W, stands for different functions distinguished by their argument structure. The multiplicative relationships involving conditional probability become additive relationships involving conditional information, as we can see by the following:

$$W(\bar{\varphi}, \mathfrak{D}) = W(\bar{\varphi} \mid \mathfrak{D}) + W(\mathfrak{D})$$

$$= W(\mathfrak{D} \mid \bar{\varphi}) + W(\bar{\varphi}) \quad ,$$

with any one of the conditional or single variable information functions being expressible in terms of the other three. These are the basic mathematical elements to be used in the construction of the optimization function.

One small obstacle remains, the fact that all these information functions involve $\bar{\sigma}$ and $\mathfrak{D}$ instead of φ and $\mathfrak{D}$ as required by the unfolding processor. The arguments $\bar{\varphi}$ and $\mathfrak{D}$ are reasonable starting points for any theoretical investigation of the information flow process, because both are firmly grounded in the physical nature of the source in question and of the spectrometer and therefore lead to physically motivated probability distributions and information functions, while φ is a synthetic object, a construction of the unfolding processor. There are no physically motivated probability distributions or information functions involving φ, except those generated by fiat.

Here is that fiat. If the distributions involving $\bar{\sigma}$ and $\mathfrak{D}$ were known, it would be possible to construct a Monte Carlo unfolding processor which, using the known distributions of $\bar{\sigma}$ and $\mathfrak{D}$, generated random φ in such a way that all probability distributions or information functions involving φ and $\mathfrak{D}$ were the same as those involving $\bar{\sigma}$ and $\mathfrak{D}$. This would be a processor different from the optimizing processor, because its output would be random, but it is valuable

conceptually because it represents a probabilistic inverse of the spectrometer measurement process, the image distribution for given data, $f(\varphi \mid \mathfrak{D})$, being the same as the object distribution, $f(\bar{\varphi} \mid \mathfrak{D})$ for that data. Therefore, let all distributions involving φ be generated from those involving $\bar{\varphi}$ by the replacement rule $\bar{\varphi} \rightarrow \varphi$.

To return to the determination of the optimum image, the optimum image is that image function which corresponds to the most probable object function for the observed data. It is therefore the image function that minimizes the conditional information of φ-if-$\mathfrak{D}$, $W(\varphi \mid \mathfrak{D})$. This is a straightforward and precise statement of the principle of unfolding which combines the previously mentioned principle of optimization with a specific form of the W-criterion.

The construction of $W(\varphi \mid \mathfrak{D})$ by direct consideration of the conditional probability of $\bar{\varphi}$-if-$\mathfrak{D}$ is usually impossible. Theoretical models generally follow the true direction of information flow, that is not from $\mathfrak{D}$ to $\bar{\varphi}$, but from $\bar{\varphi}$ to $\mathfrak{D}$. Remember that $f(\mathfrak{D} \mid \bar{\varphi})$ is the distribution and therefore $W(\mathfrak{D} \mid \bar{\varphi})$ the information function which contains a (usually linear) mathematical model of the spectrometer response as well as of the statistical fluctuations. This requires consideration of the conditional distribution of data $\mathfrak{D}$ while the object function is held fixed, a point that will become less abstract when we consider in Section 4 a specific form for the information function. To do this we use the relationships among the conditional and single variable information functions to write

$$W(\varphi \mid \mathfrak{D}) = W(\mathfrak{D} \mid \varphi) + W(\varphi) - W(\mathfrak{D}) \quad .$$

Since the minimization of $W(\varphi \mid \mathfrak{D})$ occurs by varying φ, the information function $W(\mathfrak{D})$ acts like a constant and may be dropped. Then

$$W = W(\mathfrak{D} \mid \varphi) + W(\varphi)$$

is the function that is minimized.

One of the nicest properties of the information function W, consistent with intuition and easy to remember, is its additivity. The form of W, a sum of two terms, may be interpreted as meaning that information comes from two sources. The function $W(\mathfrak{D} \mid \varphi)$ is often called the a posteriori information, and represents information that became available upon measurement. As φ varied from its initial form toward the minimum of $W(\mathfrak{D} \mid \varphi)$, and in many iterational techniques this means from a relatively structureless form to a sharply varying spectrum, φ is brought closer and closer toward consistency with data $\mathfrak{D}$. Consistency is a good thing to a degree, but beyond some limit φ ceases to acquire meaningful detail from $\mathfrak{D}$ and instead acquires noise. Since the spectrometer introduces blurring of $\mathfrak{D}$ relative to φ, and since $W(\mathfrak{D} \mid \varphi)$ is constructed in such a way that φ is consistent with $\mathfrak{D}$ when it is relatively sharp with respect to $\mathfrak{D}$, φ contains high spatial frequency components and is extremely susceptible to the acquisition of noise. This is where $W(\varphi)$ comes in. We know from our understanding of physics that it is extremely unlikely for noisy random fluctuations and typical source spectra to look alike. There is a certain range of reasonable spectral shapes. This is information represented by $W(\varphi)$,

important information such as the tendency for peaks to assume a Gaussian variation. This is a priori information, known prior to measurement. The total information is the sum of information known before and independently of the measurement and information acquired upon measurement.

To expand on the point raised in the preceding paragraph concerning consistency with the data, an image is consistent with its associated data if it predicts that the data is probable, that is, if knowledge of the camera response and the nature of the statistical counting fluctuations leads from an object like the proposed image to a data set close or similar to the observed data set. Than an understanding of the spectrometer response and the distribution of fluctuations allows one to assume an object spectrum and compute the probability of a given data set will be discussed further in the next section. The negative logarithm of this probability is the a posteriori information. It is a function of the estimated image φ and the data $\mathfrak{D}$, but also of the size of the data fluctuations and of the instrumental response. The more probable the observed data, the more consistent the estimated image, and the smaller the value of a posteriori information. A value of a posteriori information can be chosen such that all spectra with a posteriori information smaller than this value are considered consistent and all images with a posteriori information greater than this value are considered inconsistent. This defines a geometric region of consistency within the space of possible images.

This is not quite true, due to a geometrical condition present in high-dimensional spaces such as the high-dimensional data space, but with no analog in the three-dimensional space our intuition is based upon. In a high-dimensional space nearly all the volume of a smoothly bounded region is concentrated at the boundary of the region. It is as if all solid objects had nothing inside. This may sound strange, but its truth is easily demonstrated in the case of an n-dimensional sphere. If the volume of an n-dimensional sphere is obtained by integrating the volume of a series of infinitesimally thin concentric shells, the result is

$$V = \alpha \int_0^r r^{n-1}\, dr \quad ,$$

where α is a constant. The contribution of any infinitesimal shell, $\alpha r^{n-1} dr$, rises extremely rapidly with radius because r is raised to a high power. For a 100-dimensional vector data, 99 percent of the spherical volume is concentrated within the outermost 1 percent of radius! This effect is sometimes known as "the curse of many dimensions". Its consequence is the concentration of nearly all data sets for a given true $\bar{\varphi}$ at the boundary of the region of consistency.

The information value determining this boundary can be deduced from the random properties of the a posteriori information function. If some fixed, known $\bar{\varphi}$ generates an ensemble of data sets by an ensemble of separate measurements, all of the generated data sets are known to be consistent with $\bar{\varphi}$ by the very nature of the experiment,

but some will appear to be inconsistent with a large a posteriori information value, due to statistical fluctuations in $\mathfrak{D}$. After all, the a posteriori information, being a function of the random variable $\mathfrak{D}$, is itself a random variable. On the average, some expectation value $\langle W(\mathfrak{D}|\bar{\varphi})\rangle$ will be attained. In addition, $W(\mathfrak{D}|\bar{\varphi})$ acts as a radius, defining shells in $\mathfrak{D}$-space of the form

$$W_1 \leq \langle W(\mathfrak{D}\,|\,\bar{\varphi})\rangle \leq W_1 + dW_1 \quad ,$$

so that as a consequence of the curse of many dimensions it is a good approximation to say

$$W(\mathfrak{D}\,|\,\bar{\varphi}) = \langle W(\mathfrak{D}\,|\,\bar{\varphi})\rangle \quad .$$

The chance of this equality failing to a given accuracy diminishes rapidly with increasing dimensionality.

In the light of this nonintuitive behavior at high dimensionality, some statements concerning consistency with the data should be reviewed and revised. In the optimization, as φ is varied from its initial form toward the minimum of $W(\mathfrak{D}|\varphi)$, which in many iterational techniques means from a relatively structureless form to a detailed image, φ is probable brought closer and closer toward consistency with the measured data $\mathfrak{D}$ until

$$W(\mathfrak{D}\,|\,\bar{\varphi}) = \langle W(\mathfrak{D}\,|\,\bar{\varphi})\rangle \quad .$$

[Since $\bar{\varphi}$ is unknown, $\langle W(\mathfrak{D}|\bar{\varphi})\rangle$ can be approximated by $\langle W(\mathfrak{D}|\varphi)\rangle$. Anyway it is usually found to be approximately constant, independent of $\bar{\varphi}$.] Beyond this, further optimization of $W(\mathfrak{D}|\varphi)$ is fruitless,

because φ probably becomes less consistent with $\mathfrak{D}$. As a result the optimization of $W(\mathfrak{D}\,|\,\varphi)$ alone would end with φ confined to a subspace of the space of all possible φ defined by the expectation value of the a posteriori information. That is, φ would not be uniquely determined.

A random choice of φ from the subspace of φ-space defined by the equation

$$W(\mathfrak{D}\,|\,\varphi) = \langle W(\mathfrak{D}\,|\,\overline{\varphi})\rangle \quad ,$$

would be most unsatisfactory. The noise magnification resulting from resolution enhancement would obliterate all recognizable features. Good spectra are present within the subspace, but they represent an extremely small fraction of the total region. It is the function of a priori information functions to locate these small regions. The combined optimization of

$$W = W(\mathfrak{D}\,|\,\varphi) + W(\varphi)$$

results in the minimization of $W(\varphi)$ within the region of consistency. If $W(\varphi)$ is constructed to minimize for the desired class of spectra, the desired selection will be achieved.

The a posteriori information, $W(\mathfrak{D}\,|\,\varphi)$, determines the region of consistent spectra, and the a priori information, $W(\varphi)$, determines the most regular spectrum within the region of consistency. As a practical matter, it is relatively easy to construct a form of $W(\varphi)$ that prejudices toward regular images, and relatively difficult to

normalize it so that its relative strength in W is exactly that required to pull $W(\mathfrak{D}|\varphi)$ to its expectation value. Therefore, it is more direct to state the optimization problem as

$$\text{minimize} \quad W(\varphi)$$

$$\text{subject to} \quad W(\mathfrak{D} \mid \varphi) = \langle W(\mathfrak{D} \mid \overline{\varphi}) \rangle \quad .$$

On the other hand it is relatively difficult to implement a constrained optimization like this, and relatively easy to implement a simple or unconstrained optimization. Two methods have been developed for converting the constrained optimization to an unconstrained one. In the first method the function that is minimized has the form

$$W = \frac{1}{\epsilon}\left\{W(\mathfrak{D} \mid \varphi) - \langle W(\mathfrak{D} \mid \overline{\varphi}) \rangle\right\}^2 + \epsilon\left\{W(\varphi)\right\}^2 \quad ,$$

where ϵ is a smaller number. The first term dominates until the a posteriori information approaches its expectation, after which the minimization of the a priori information dominates. In the second method, the method of Lagrange multipliers, the function that is minimized has the form

$$W = W(\mathfrak{D} \mid \varphi) + \lambda\, W(\varphi) \quad ,$$

where λ is the Lagrange multiplier. Generally, the value attained by $W(\mathfrak{D}|\varphi)$ increases as λ increases, causing $W(\varphi)$ to pull the optimum φ away from the value that would minimize $W(\mathfrak{D}|\varphi)$. Therefore, the Lagrange multiplier can be adjusted as part of the optimization, to the value required to fulfill the expectation value condition.

3. OPTIMIZATION CRITERIA

The optimization function used in MAZE 2 is designed to produce regular, positive spectral images, with minimal alteration of the true widths of Gaussian peaks. MAZE3 is similar in that sense. In this section we describe the specific form of this function.

An NC-dimensional energy grid structure is assumed in which the width of the J-th energy bin is $\Delta E(J)$, for $J=1,\ldots,NC$. This structure is specified by an (NC+1)-dimensional bin-edge vector, $E(J)$, $J=1,\ldots,(NC+1)$. The quantities that are estimated are the probabilities of occurrence of flux in the J-th energy channel, an NC-dimensional vector, $Q(J)$. This vector is related to the image spectrum, $\varphi(E)$, of the previous chapter by the equation

$$Q(J) = \int_{E(J)}^{E(J+1)} \varphi(E)\, dE \quad . \tag{3.1}$$

The probability, $Q(J)$ is an integral quantity, roughly proportional to the width of the J-th energy bin, while the image spectrum, $\varphi(E)$, is a differential quantity, indeperdent of the energy grid structure.

Actually, $Q(J)$ is a 2*NC-dimensional vector where the indices $J=1,\ldots,NC$ refer to the continuum (Q_C) and indices $J=NC+1,\ldots,2*NC$ refer to the discrete (Q_D) portion of the spectrum. The subscripts C and D will be explicitly indicated wherever needed, otherwise it

will be assumed that Q refers to both the continuum and the discrete elements of the probability vector of dimension 2*NC. Then $Q_D(J)$ is actually Q(NC+J).

There is an NR-dimensional data vector, C(I), for I = 1, . . . , NR. It is assumed to be linearly related to the spectral estimate, Q, by the response matrix, A, in the folding equation

$$C(I) + \delta C(I) = \sum_J A(I,J) * (Q(J) + \delta Q(J)) \quad . \tag{3.2}$$

The symbol δC represents statistical fluctuations of the data vector. In Section 3.1, in which the basic optimization function is described, C is assumed to have been obtained by a simple counting process so that δC is distributed according to the multinomial distribution. The assumption is not generally valid, but it is generally possible to transform the problem to a form in which the multinomial assumption yields good solutions. This is the equivalent count form, which is discussed in Section 3.3. Also part of the equivalent count form is the condition

$$\sum_{J=1}^{NC} \left\{ Q_C(J) + Q_D(J) \right\} = 1 \tag{3.3}$$

representing the assumption that all flux of interest passes through the defined energy grid structure. The problem is worked under condition (3.3) and restored upon completion to the normalization specified by condition (3.1). This is discussed in mathematical detail in this section. The symbol δQ represents error in the image spectrum relative to the object spectrum.

The W-criterion is dependent on the arguments (Q;C, A, E, NR, NC) and has the form discussed in Section 2. A restatement of the variable information function in terms of these arguments, has the form

$$W(Q;C, A, E, NR, NC) = W_1(Q;C, A, NR, NC)$$

$$+ \tau_C W_2(Q_C;E, NC)$$

$$+ \tau_D W_2(Q_D;E, NC)$$

where W_1 is the a posteriori and W_2 the a priori information. These will be treated in detail in the following subsections.

3.1 THE A POSTERIORI INFORMATION

The form of the a posteriori information W_1 was derived from multinomial statistics. According to multinomial statistics the probability for C counts distributed in NR channels is:

$$PROB = \{COUNTS!\} \sum_{I=1}^{NR} \frac{P(I)^{C(I)}}{C(I)!} \quad .$$

where

$$P(I) = \sum_{J=1}^{NC} A(I, J) * \left\{Q_C(J) + Q_D(J)\right\} \quad . \qquad (3.1.1)$$

The construction of an information function as the negative logarithm of a probability distribution was discussed in Section 2, whereupon it follows that

$$W_1 = - \sum_{I=1}^{NR} C(I) * \ell n\ P(I) - K \qquad (3.1.2)$$

The constant, K, which does not affect W_1 as a function of Q, has the form

$$K = \ell n\ (COUNTS!) - \sum_{I=1}^{NR} \ell n\ C(I) \quad .$$

Using Stirling's approximation

$$\ell n(X!) = X\ \ell n\ X - X$$

it can be brought to the form

$$K = \sum_{I=1}^{NR} C(I) * \{\ell n\ (COUNTS) - \ell n\ C(I)\} \quad .$$

Substituting this back into W_1 in Equation 3.1.2 and combining log terms, we find

$$W_1(Q;C, A, NR, NR) = - \sum_{I=1}^{NR} C(I) * \ell n\ \frac{COUNTS*P(I)}{C(I)} \quad .$$

The form of the multinomial distribution assumes that the NR-dimensional vector P is the probability for all possible channels of detection. Otherwise there would effectively be an (NR+1)-th data channel for events not received by the first NR channels. This can be stated mathematically as the condition

$$1 = \sum_{I=1}^{NR} P(I) \quad . \tag{3.1.3}$$

It has the same form as the previously mentioned condition (3.3), and is directly related to it. Combining Equations 3.1.1 and 3.1.3, we get

$$1 = \sum_{I=1}^{NR} P(I) = \sum_{I=1}^{NR} \sum_{J=1}^{NC} A(I,J) * \left\{ Q_C(J) + Q_D(J) \right\} \quad .$$

Then, reversing the order of summation, this becomes

$$1 = \sum_{J=1}^{NC} \left\{ Q_C(J) + Q_D(J) \right\} \sum_{I=1}^{NR} A(I,J) \quad . \tag{3.1.4}$$

In Section 3.3 it will be shown that in the equivalent count form the summation of A over I, a summation of the columns of the response matrix, gives the result

$$\sum_{I=1}^{NR} A(I,J) = 1 \quad .$$

Therefore Equation 3.1.4 reduces to condition 3.3.

Condition 3.3 constitutes a one-dimensional constraint on the domain of optimization, leaving Q_C and Q_D with (NC-1) degrees of freedom. In this constraint region the calculus of variations provides an expression for the minimum of W_1. Taking the variation of W_1 with respect to P gives

$$\delta W_1 = \sum_{I=1}^{NR} \frac{\delta W_1}{\delta P(I)} \delta P(I) = - \sum_{I=1}^{NR} \frac{C(I)}{P(I)} \delta P(I) \quad . \qquad (3.1.5)$$

The variation of the constraint Equation 3.1.3 gives

$$\delta \sum_{I=1}^{NR} P(I) = \sum_{I=1}^{NR} \delta P(I) = 0 \quad . \qquad (3.1.6)$$

Using the method of Lagrange multipliers, the minimum is described by

$$\delta W_1 + \lambda \delta \sum_{I=1}^{NR} P(I) = 0 \quad ,$$

where the Lagrange multiplier λ is to be determined. Substituting 3.1.5 and 3.1.6 into this equation, it becomes

$$\sum_{I=1}^{NR} \left\{ - \frac{C(I)}{P(I)} + \lambda \right\} \delta P(I) = 0 \quad .$$

Because the $\delta P(I)$ are independent, we set each coefficient to zero independently, and find

$$P(I) = \frac{C(I)}{\lambda} \quad , \tag{3.1.7}$$

the Lagrange multiplier being evaluated by summing over I. Performing this summation,

$$\sum_{I=1}^{NR} P(I) = 1 = \sum_{I=1}^{NR} \frac{C(I)}{\lambda} = \frac{COUNTS}{\lambda} \quad ,$$

from which $\lambda = COUNTS$, and

$$P(I) = \frac{C(I)}{COUNTS} \quad . \tag{3.1.8}$$

This agrees with the notion that $P(I)$ is the probability for a count in channel I. Substituting this $P(I)$ back into W_1, the minimum value of W_1 is found to be zero.

A form of W_1 in which constraint 3.1.3 is implicit is useful for the accelerated steepest descent technique used in MAZE. It may be derived by considering an $(NR+1)$-th dummy channel, channel 0, with $P(0) \approx 1$ so that

$$\sum_{I=1}^{NR} P(I) << 1 \quad .$$

Then, $P(I)$ for $I \neq 0$ is far removed from the effect of the constraint condition and can vary freely. The minimum of W_1 with respect to

$$\sum_{I=1}^{NR} P(I)$$

is controlled by the choice of $C(0)$. To preserve the magnitude of $P(I)$, the probability of a count in channel I can be defined as $\alpha P(I)$, where $\alpha \to 0$. Omitting the constant term from Equation 3.1.2, W_1 becomes

$$W_1 = - C(0) * \ell n\ P(0) - \sum_{I=1}^{NR} C(I) * \ell n\ \alpha P(I) \quad .$$

The count total becomes $C(0)$ + COUNTS, and constraint 3.1.3 becomes

$$P(0) + \alpha \sum_{I=1}^{NR} P(I) = 1 \quad . \qquad (3.1.9)$$

According to Equation 3.1.7 obtained by calculus of variations, the minimum of W_1 occurs at the P values

$$\begin{cases} P(0) = \dfrac{C(0)}{C(0) + \text{COUNTS}} \quad , \\ \\ \alpha P(I) = \dfrac{C(I)}{C(0) + \text{COUNTS}} \quad . \end{cases}$$

The latter expression must agree with the original minimum 3.1.8, so $C(0)$ must be set to

$$C(0) = \frac{1-\alpha}{\alpha} * \text{COUNTS} \quad .$$

Using this expression for $C(0)$ and the constraint condition, Equation 3.1.9, the a posteriori information W_1 becomes

$$W_1 = - \frac{1-\alpha}{\alpha} * \text{COUNTS} * \ell n \left\{ 1 - \alpha \sum_{I=1}^{NR} P(I) \right\} - \sum_{I=1}^{NR} C(I) * \ell n \, \alpha P(I) \quad .$$

In the limit $\alpha \to 0$ the first ℓn term is well approximated by a first order expansion

$$\ell n \left\{ 1 - \alpha \sum_{I=1}^{NR} P(I) \right\} \approx - \alpha \sum_{I=1}^{NR} P(I) \quad .$$

Substituting this back into the equation for W_1, replacing $\alpha P(I)$ by its original form, $P(I)$, and taking the limit as $\alpha \to 0$, W_1 becomes

$$W_1 = \text{COUNTS} * \sum_{I=1}^{NR} P(I) - \sum_{I=1}^{NR} C(I) * \ell n \, P(I) \quad .$$

This is the implicit constraint form of W_1. With this form the minimum of W_1 occurs at the equation given by 3.1.8 without Lagrange multipliers.

3.2 THE A PRIORI INFORMATION

The a priori information W_2 is designed to suppress oscillations but not Gaussian peaks. Since oscillations are accompanied by

large derivative terms, the reduction of almost any low order derivative function will reduce oscillations. Gaussian peaks also contribute certain large derivative terms, and a careless choice of W_2 will cause Gaussian peaks to be smeared. Since a compromise is affected between smoothing and conformity to the data, the practical result of using a bad W_2 is oscillations near Gaussian peaks appearing as subsidiary peaks and possible negative fluxes, and smearing of the true peak. For this reason, care must be exercised to construct a derivative expression that leaves Gaussian peaks intact.

The a priori information functions have the form

$$W_2(Q_C;E,NC) = \tfrac{1}{2}\sum_{J=1}^{NC}\left[\frac{d\ell n\,\varphi_C(E_J)}{dE}\right]^2$$

$$W_2(Q_D;E,NC) = \tfrac{1}{2}\sum_{J=1}^{NC}\left[\frac{d^2\ell n\varphi_D(E_J)}{dE^2}\right]^2$$

for the continuum and discrete spectra respectively. The derivative forms are approximately independent of the properties of the Gaussian peaks. Thus, minimization results in regularization without alteration of the peaks. The E_J is an energy representative of the J-th energy bin and the derivatives are in terms of channels. It is assumed that energy is linear as a function of channel which is a good approximation for germanium detectors.

These forms may be written approximately as

$$W_2 = \tfrac{1}{2} \sum_{J=1}^{NC} \left(\sum_{K=1}^{NC} D_\alpha(J,K) * \log \text{PHI}(K) \right)^2$$

where α is to be replaced by C or D for the continuum or the discrete parts respectively. Also, $\phi(E_K)$ has been replaced by PHI(K). D_C and D_D are matrices as will be shown below.

Another form of this equation is:

$$W_2 = \tfrac{1}{2} \sum_{J=1}^{NC} \sum_{K=1}^{NC} \log \text{PHI}(J) * D_\alpha D_\alpha(J,K) * \log \text{PHI}(K)$$

where

$$D_\alpha D_\alpha(J,K) = \sum_{L=1}^{NC} D_\alpha(L,J) * D_\alpha(L,K) = D_\alpha^T * D_\alpha$$

and, again, α is to be replaced by C or D.

The matrix D_α is independent of PHI and can be calculated once and for all. For the first derivative we have the following:

$$
D_C^T * D_C = \begin{bmatrix}
0 & -1 & 0 & 0 & & & & \\
0 & 1 & -1 & 0 & & & & \\
0 & 0 & 1 & -1 & & & & \\
0 & 0 & 0 & 1 & & & & \\
 & & & & \ddots & & & \\
 & & & & 1 & -1 & 0 & 0 \\
 & & & & 0 & 1 & -1 & 0 \\
 & & & & 0 & 0 & 1 & -1 \\
 & & & & 0 & 0 & 0 & 1
\end{bmatrix}
$$

$$
* \begin{bmatrix}
0 & 0 & 0 & 0 & & & & \\
-1 & 1 & 0 & 0 & & & & \\
0 & -1 & 1 & 0 & & & & \\
0 & 0 & -1 & 1 & & & & \\
 & & & & \ddots & & & \\
 & & & & 1 & 0 & 0 & 0 \\
 & & & & -1 & 1 & 0 & 0 \\
 & & & & 0 & -1 & 1 & 0 \\
 & & & & 0 & 0 & -1 & 1
\end{bmatrix}
$$

$$
= \begin{bmatrix}
1 & -1 & 0 & 0 & & & & \\
-1 & 2 & -1 & 0 & & & & \\
0 & -1 & 2 & -1 & & & & \\
0 & 0 & -1 & 2 & & & & \\
 & & & & \ddots & & & \\
 & & & & 2 & -1 & 0 & 0 \\
 & & & & -1 & 2 & -1 & 0 \\
 & & & & 0 & -1 & 2 & -1 \\
 & & & & 0 & 0 & -1 & 1
\end{bmatrix}
$$

which turns out to be an approximation to the second derivative. The other off-diagonal elements are zero.

Similarly, for the second derivative:

$$
D_D^T * D_D = \begin{bmatrix}
-1 & 0 & 0 & 0 & & & & \\
1 & -2 & 1 & 0 & & & & \\
0 & 1 & -2 & 1 & & & & \\
0 & 0 & 1 & -2 & & & & \\
 & & & & \ddots & & & \\
 & & & & -2 & 1 & 0 & 0 \\
 & & & & 1 & -2 & 1 & 0 \\
 & & & & 0 & 1 & -2 & 1 \\
 & & & & 0 & 0 & 1 & -1
\end{bmatrix}
$$

$$
* \begin{bmatrix}
-1 & 1 & 0 & 0 & & & & \\
1 & -2 & 1 & 0 & & & & \\
0 & 1 & -2 & 1 & & & & \\
0 & 0 & 1 & -2 & & & & \\
 & & & & \ddots & & & \\
 & & & & -2 & 1 & 0 & 0 \\
 & & & & 1 & -2 & 1 & 0 \\
 & & & & 0 & 1 & -2 & 1 \\
 & & & & 0 & 0 & 1 & -1
\end{bmatrix}
$$

$$
= \begin{bmatrix}
2 & -3 & 1 & 0 & & & & \\
-3 & 6 & -2 & 1 & & & & \\
1 & -4 & 6 & -2 & & & & \\
0 & 1 & -4 & 6 & & & & \\
 & & & & \ddots & & & \\
 & & & & 6 & -4 & 1 & 0 \\
 & & & & -4 & 6 & -4 & 1 \\
 & & & & 1 & -4 & 6 & -3 \\
 & & & & 0 & 1 & -3 & 2
\end{bmatrix}
$$

which is an approximation to the fourth derivative. Because the D matrices are highly redundant, they need not be stored explicitly.

3.3 TRANSFORMATION TO EQUIVALENT COUNTS

The multinomial distribution has the desirable property of distributing C(I) among positive values

$$0 \leq C(I)$$

in accordance with assumptions that are reasonable for a simple event-counting process. The standard deviation of the I-th channel data may be deduced from the multinomial distribution, and has the form

$$\sigma(I) = \sqrt{COUNTS * P(I) * (1. - P(I))} \quad .$$

For multichannel data P(I) is usually sufficiently smaller than 1., to make the approximation

$$\sigma(I) = \sqrt{COUNTS * P(I)}$$

or, what is the same

$$\sigma(I) = \sqrt{\langle C(I) \rangle} \quad ,$$

where $\langle C(I) \rangle$ denotes the expectation of C(I). Therefore, the fractional error in C(I) is

$$\frac{\sqrt{\langle C(I) \rangle}}{C(I)} \quad ,$$

or, approximately,

$$\frac{1}{\sqrt{C(I)}} \quad .$$

Generally, data D(I) is inputed with error sigma (I) such that the fractional error

$$\frac{SIGMA(I)}{D(I)}$$

is not equal to the multinomial value

$$\frac{1}{\sqrt{D(I)}} \quad .$$

However, if a pseudocount vector C(I) is constructed from D(I) and SIGMA(I) according to the prescription

$$C(I) = \left[\frac{D(I)}{SIGMA(I)}\right]^2 \quad ,$$

then the pseudocount vector will have the desired fractional error.

Now let us consider the ramifications of the pseudocount definition. Suppose V is a vector that folds to D:

$$D(I) = \sum_{J=1}^{NC} A(I,J) * V(J) \quad .$$

If a new response matrix is defined by the transformation

$$A(I,J) \rightarrow A(I,J) = \frac{C(I)}{D(I)} A(I,J) \quad , \qquad (3.3.1)$$

then V will fold to C:

$$C(I) = \sum_{J=1}^{NC} A(I, J) * V(J) \quad .$$

If A is again redefined by the transformation

$$A(I, J) \rightarrow A(I, J) = \frac{A(I, J)}{\sum_{I=1}^{NR} A(I, J)} \tag{3.3.2}$$

and V by the inverse transformation

$$V(J) \rightarrow V(J) = \left\{ \sum_{I=1}^{NR} A(I, J) \right\} V(J) \quad , \tag{3.3.3}$$

then the new A will have the property that

$$\sum_{I=1}^{NR} A(I, J) = 1 \quad .$$

Upon input to the program, pseudocount vector C is calculated, and A is converted to the equivalent count form defined by (3.3.1) and (3.3.2). The spectral estimate therefore contains the vector multiplier seen on the right side of (3.3.3). Upon conclusion of the calculation, this multiplier is divided out and A is restored to its original form.

4. IMPLEMENTATION OF THE OPTIMIZATION

The minimization of W is accomplished by an accelerated steepest descent moving in the space of ℓnQ. To understand this, consider first the simple steepest descent, an iterational technique which generates a sequence of points $Q^{(1)}, Q^{(2)}, \ldots, Q^{(m)}, \ldots$ that approaches the minimum of W. The method is known by knowing the starting point, $Q^{(1)}$, and a rule for the transition $Q^{(m)} \rightarrow Q^{(m+1)}$. The starting point is taken to be that Q for which the image spectrum is constant or flat. This choice assures that any structure that appears in $Q^{(m)}$ comes only from the form of W and not from the choice of $Q^{(1)}$. The rule for the transition $Q^{(m)} \rightarrow Q^{(m+1)}$ takes the form

$$\ell nQ_\alpha^{(m)}(J) \rightarrow \ell nQ_\alpha^{(m+1)}(J) = \ell nQ_\alpha^{(m)}(J) + t_\alpha \Delta^{(m)}(J)$$

or, equivalently,

$$Q_\alpha^{(m)}(J) \rightarrow Q_\alpha^{(m+1)}(J) = Q_\alpha^{(m)}(J)\ e^{t_\alpha \Delta^{(m)}(J)} \tag{4.1}$$

where α has the same interpretation as in the previous section. The direction of the transition $\Delta^{(m)}$ is the direction of steepest descent. The gradient of W with respect to $\ell nQ_\alpha(J)$ is

$$\Delta^{(m)}(J) = \frac{\partial W}{\partial\, \ell nQ(J)} \quad .$$

The gradient of W_1 in the implicit constraint form is

$$\frac{\partial W_1}{\partial \ell n Q(J)} = \left\{ Q_C(J) + Q_D(J) \right\} * \sum_{I=1}^{NR} \left\{ C(I) - A(I,J) * \frac{C(I)}{P(I)} \right\} . \quad (4.2)$$

The gradient of W_2, from Section 3.2 is

$$\frac{\partial W_2}{\partial \ell n Q_\alpha(J)} = Q_\alpha(J) * \sum_{k=1}^{NC} D_\alpha D_\alpha(J,K) * \ell n \, PHI(K) ,$$

where

$$\frac{\partial W_2}{\partial \ell n Q_\alpha(J)} = \frac{\partial W_2}{\partial \ell n \, PHI(J)}$$

because $Q_\alpha(J)$ differs from $PHI(J)$ by only a constant multiplier. Since $\Delta^{(m)}$ is a direction, it may be multiplied by any constant, and we take

$$\Delta^{(m)}(J) = \frac{1}{COUNTS} \left\{ \frac{\partial W_1}{\partial \ell n \, Q(J)} + \tau_C \frac{\partial W_2}{\partial \ell n Q_C(J)} + \tau_D \frac{\partial W_2}{\partial \ell n Q_D(J)} \right\}$$

This choice keeps the components of $\Delta^{(m)}$ closer to the value one.

Expanding W in a second order Taylor expansion in $Q_\alpha(J)$ about $Q_\alpha^{(m)}(J)$ gives a quadratic dependence with t_α in the direction $\Delta^{(m)}$. We let $Q^{(m)}(J)$ become $Q^{(m+1)}(J)$ by the process (4.1) and the deviation in $Q_\alpha(J)$ is

$$Q_\alpha^{(m+1)}(J) - Q_\alpha^{(m)}(J) = Q_\alpha^{(m)}(J) * \left\{ e^{t_\alpha \Delta^{(m)}(J)} - 1 \right\} .$$

Since $t_\alpha \Delta^{(m)}(J)$ is assumed to be small, we expand the exponential to the first order, and find, approximately,

$$Q_\alpha^{(m+1)}(J) - Q_\alpha^{(m)}(J) = Q_\alpha^{(m)}(J) * t_\alpha \Delta^{(m)}(J) \quad . \tag{4.3}$$

Therefore, the second order Taylor expansion of W becomes

$$W\left(Q_\alpha^{(m+1)}(J)\right) = W\left(Q_\alpha^{(m)}(J)\right)$$

$$+ t_\alpha \sum_{J=1}^{NC} \frac{\partial W}{\partial Q_\alpha(J)} Q_\alpha^{(m)}(J) \Delta^{(m)}(J)$$

$$+ \tfrac{1}{2} \sum_{J,K=1}^{NC} \Delta^{(m)}(J) Q_\alpha^{(m)}(J) \frac{\partial^2 W}{\partial Q_\alpha(J) \partial Q_\beta(K)} \Delta^{(m)}(K) Q_\beta^{(m)}(K) t_\alpha t_\beta \tag{4.4}$$

The derivatives are evaluated at $Q_\alpha^{(m)}(J)$ and β has the same meaning as α.

The minimum of approximation 4.4 occurs where

$$\frac{\partial W}{\partial t_\alpha} = 0 \quad . \tag{4.5}$$

Since W is approximated by 4.4 as quadratic in t_α, 4.5 is a linear equation in t_α, which can be solved to obtain t_α, the appropriate

step length for the $(m) \rightarrow (m+1)$ iteration. However, approximation 4.3 holds only if $t_\alpha \Delta^{(m)}(J)$ is small with respect to the value 1. Otherwise, the argument leading to 4.5 breaks down. To prevent this, we modify 4.5 to the following:

$$\frac{\partial}{\partial t_\alpha} \left\{ W + \tfrac{1}{2} \sum_{J=1}^{NC} \left[\frac{t_\alpha \Delta^{(m)}(J)}{.5} \right]^2 \right\} \quad . \tag{4.6}$$

The additional term is a chi-squared expression with $t_\alpha \Delta^{(m)}(J)$ having a mean of zero and a standard deviation of 0.5 about zero. Therefore, 4.6 contains both a tendency to minimize W and, in balance, a tendency to hold approximation 4.3 within its range of validity.

To obtain the step length, t_α, we combine 4.4 and 4.6. Then,

$$t_{D,C} = - \left\{ \sum_{J,K=1}^{NC} \Delta^{(m)}(J)\, Q_\alpha^{(m)}(J)\, \frac{\partial^2 W}{\partial Q_\alpha(J)\, \partial Q_\beta(K)}\, \Delta^{(m)}(K)\, Q_\beta^{(m)}(K) \right.$$

$$\left. + \sum_{J=1}^{NC} \left| \Delta^{(m)}(J) \right|^2 \right\}^{-1} * \left\{ \sum_{J=1}^{NC} \frac{\partial W}{\partial Q_D}\, Q_D^{(m)}\, \Delta^{(m)}(J), \right.$$

$$\left. \sum_{J=1}^{NC} \frac{\partial W}{\partial Q_C}\, Q_C^{(m)}(J)\, \Delta^{(m)}(J) \right\}^T \tag{4.7}$$

where the first term in brackets is a 2 x 2 matrix and the second term is a vector. The first derivative has already been expressed in Equation 4.2. The second derivative has the form

$$\frac{\partial^2 W}{\partial Q_\alpha(J)\partial Q_\beta(K)} = \sum_{I=1}^{NR} \frac{C(I)}{P(I)**2} A(I,J)\, A(I,K) + \tau_\alpha \frac{D_\alpha D_\beta(J,K)}{Q_\alpha(J) Q_\beta(K)} \qquad (4.8)$$

where α and β take on values C and D in turn. The two bracketed terms of 4.7 are obtained from the derivative expressions by performing the summations indicated in 4.7, a straightforward algebraic manipulation. When the first term of the second derivative 4.8 containing an I-summation is combined with the J, K-summation in 4.7, a triple summation results:

$$\sum_{J,K=1}^{NC} \Delta^{(m)}(J)\, Q_\alpha^{(m)}(J) \sum_{I=1}^{NR} \frac{C(I)}{P(I)**2} A(I,J)\, A(I,K)\, \Delta^{(m)}(K)\, Q_\alpha^{(m)}(K) \quad .$$

This would be a time-consuming operation, but fortunately it can be reduced to a double summation

$$\sum_{I=1}^{NR} \frac{C(I)}{P(I)**2} \left(\sum_{J=1}^{NC} A(I,J) \left| Q_C(J) + Q_D(J) \right| \Delta^{(m)}(J) \right)^2 \quad ,$$

with a consequent saving in computation time.

The preceding description of the iteration step is based upon the calculation of a direction, $\Delta^{(m)}$, according to the gradient of W, and of a path length, t_α, according to a modified quadratic approximation of W. These quantities are then used to transform the m-th spectral estimate by transition rule 4.1:

$$\ell n Q_\alpha^{(m)}(J) \rightarrow \ell n Q_\alpha^{(m+1)}(J) = \ell n Q_\alpha^{(m)}(J) + t_\alpha \Delta^{(m)}(J) \quad .$$

An acceleration process is applied to the simple gradient sequence described thus far. In the accelerated steepest descent, $\Delta^{(m)}$ alternates between the gradient form and the difference form

$$\Delta^{(m)}(J) = \ell nQ^{(m)}(J) - \ell nQ^{(m-3)}(J)$$

in the sequence gradient, gradient, gradient, difference, gradient, difference, gradient, difference ...; that is, gradient form on odd steps, difference form on even steps, except the second, which is gradient. This speeds the calculation significantly. It decouples the gradient of W from direct control of the iterational sequence, and, in effect, allows the iterational sequence to build up momentum.

In Section 2, we discussed the need for adjusting the Lagrange multiplier, called τ_α in Section 3, to obtain agreement between the value of the a posteriori information W_1 and its expectation value. This is called the outer iteration of W_1 as distinguished from the inner iteration of W that has been discussed in this section so far. A complete linear iterational sequence is executed at each stage of the outer iteration associated with a given value of τ_α.

First, let us consider the expectation value of W_1. Since W_1 is a function of the random variable C, it is itself a random variable. Expanding W_1 in C about the minimum point

$$C(I) = COUNTS * P(I) \quad ,$$

W_1 becomes

$$W_1(C(I) + \delta C(I)) \approx W_1(C(I)) + \sum_{I=1}^{NR} \frac{\partial W_1}{\partial C(I)} \delta C(I)$$

$$+ \tfrac{1}{2} \sum_{I=1}^{NR} \sum_{L=1}^{NR} \frac{\partial^2 W_1}{\partial C(I)\, \partial C(L)} \delta C(I)\, \delta C(L) \quad . \tag{4.9}$$

At the minimum point

$$W_1(C(I)) = 0 \quad .$$

The first derivative of the explicit constraint form of W is

$$\left.\frac{\partial W_1}{\partial C(I)}\right|_{C(I)=COUNTS*P(I)}$$

$$= - \ell n \left.\frac{COUNTS*P(I)}{C(I)} + 1\right|_{C(I)=COUNTS*P(I)} = 1 \; . \tag{4.10}$$

The second derivative of the explicit constraint form is

$$\left.\frac{\partial W_1}{\partial C(I)\, \partial C(L)}\right|_{C(I)=COUNTS*P(I)} = \begin{cases} \dfrac{1}{COUNTS*P(I)} & , \quad I=L \\ 0 & , \quad I \neq L \end{cases} \quad . \tag{4.11}$$

Substituting 4.10 and 4.11 in 4.9, W_1 becomes

$$W_1 = \sum_{I=1}^{NR} \delta C(I) + \tfrac{1}{2} \sum_{I=1}^{NR} \frac{\{\delta C(I)\}^2}{COUNTS*P(I)} \quad .$$

The randomness of W_1 arises from the randomness of $\delta C(I)$. If the expectation of $C(I)$ is approximated as COUNTS*P(I), the expectation of $\delta C(I)$ is zero. The expectation of $\{\delta C(I)\}^2$ is COUNTS*P(I), so the expectation of W_1 is

$$\langle W_1 \rangle = \tfrac{1}{2} NR \quad .$$

The condition

$$W_1(Q) = \text{expectation } W_1$$

can be taken as a test of the consistency of Q with the data. Several iterational sequences are executed until τ_α has a value such that

$$\text{expectation } W_1 < W_1 < 1.3 * \text{expectation } W_1 \quad .$$

This is the value which determines the adjustment of τ_α.

This adjustment process is the iterational sequence associated with the outer iteration. After each inner iterational sequence, τ_α is adjusted according to the transition rule

$$\tau_\alpha \rightarrow \tau_\alpha \frac{\langle W_1 \rangle}{W_1} \quad ,$$

τ_α getting larger if a small W_1 indicates regularization is too weak, or smaller if a large W_1 indicates regularization is too strong. If, at any point in the outer sequence, the consistency is good enough to permit the condition

$$\langle W_1 \rangle < W_1 < 1.3 \langle W_1 \rangle$$

to be obeyed, the outer iteration is terminated.

5. RESPONSE FUNCTION PARAMETERIZATION

The complete Ge(Li) spectrum unfolding turns out to be mechanically very tedious since a great deal of laboratory work has to be done in order to obtain the spectrometer response. Consequently, the potential users of the code that were contacted expressed minimal interest in a code that would fully unfold Ge(Li) spectra. However, a great deal of interest was expressed regarding a code that would superresolve peaks, since the detector measurements necessary are concerned only with line width information.

Another consideration along these lines is that the response matrix for the unfolding of Gaussian spectral lines is "nearly" diagonal. That is, the non-zero values are concentrated near the diagonal elements of the matrix. This means that a spectrum that has many channels can be sectioned into smaller, more reasonable pieces without taxing the storage capacity of most serial computers. Minimal storage capacity was not a prime requirement for the I4 system, however any actual checks on the performance of the code on actual data were of necessity limited to cases for which detector response data could be readily obtained.

One of the difficulties in Ge(Li) unfolding is the representation of the response matrix. If the unfolding problem has many channels then the matrix is very large and cannot be core contained. This

means that only parts of the matrix can be in the computer memory and the rest shuffled in and out as needed. This problem has to be dealt with in any case but for Ge(Li) detectors there is a way to parameterize the matrix in terms of certain parameters. Figure 1 is an example of a 2 MeV Ge(Li) line shape but without the Gaussian blurring on the peaks. The mathematical details of the parameterization have been worked out but will not be presented here in great detail, only conceptually.

As detailed in Chapters 1 and 2, the information function can be represented as two parts: the a posteriori and a priori as follows.

$$W = W_1[\mathfrak{D}, A_i(\beta_\ell, \lambda, \sigma, E_o)] + W_2(\beta_\ell, \lambda, \sigma, E_o) \quad , \quad \ell = 1, \ldots, 5$$

where the parameters are only the ones important in the parameterization. The arguments are as follows:

$$A_i(E_o) = A_i(\beta_\ell, \lambda, \sigma, E_o) \quad ,$$

where $A_i(E_o)$ is the response specifying the contribution to channel i from energy E_o. The β_ℓ's are the amplitude weight factors for the full energy peak, single escape peak, double escape peak, Compton continuum, and Compton edge corresponding to $\ell = 1,2,3,4,5$ respectively. λ is the logarithmic slope of the Compton edge and σ is the variance of the Gaussian distribution of the peaks. It is assumed that the variance is the same for all of the peaks. $\mathfrak{D}$ is the response data at energy E_o.

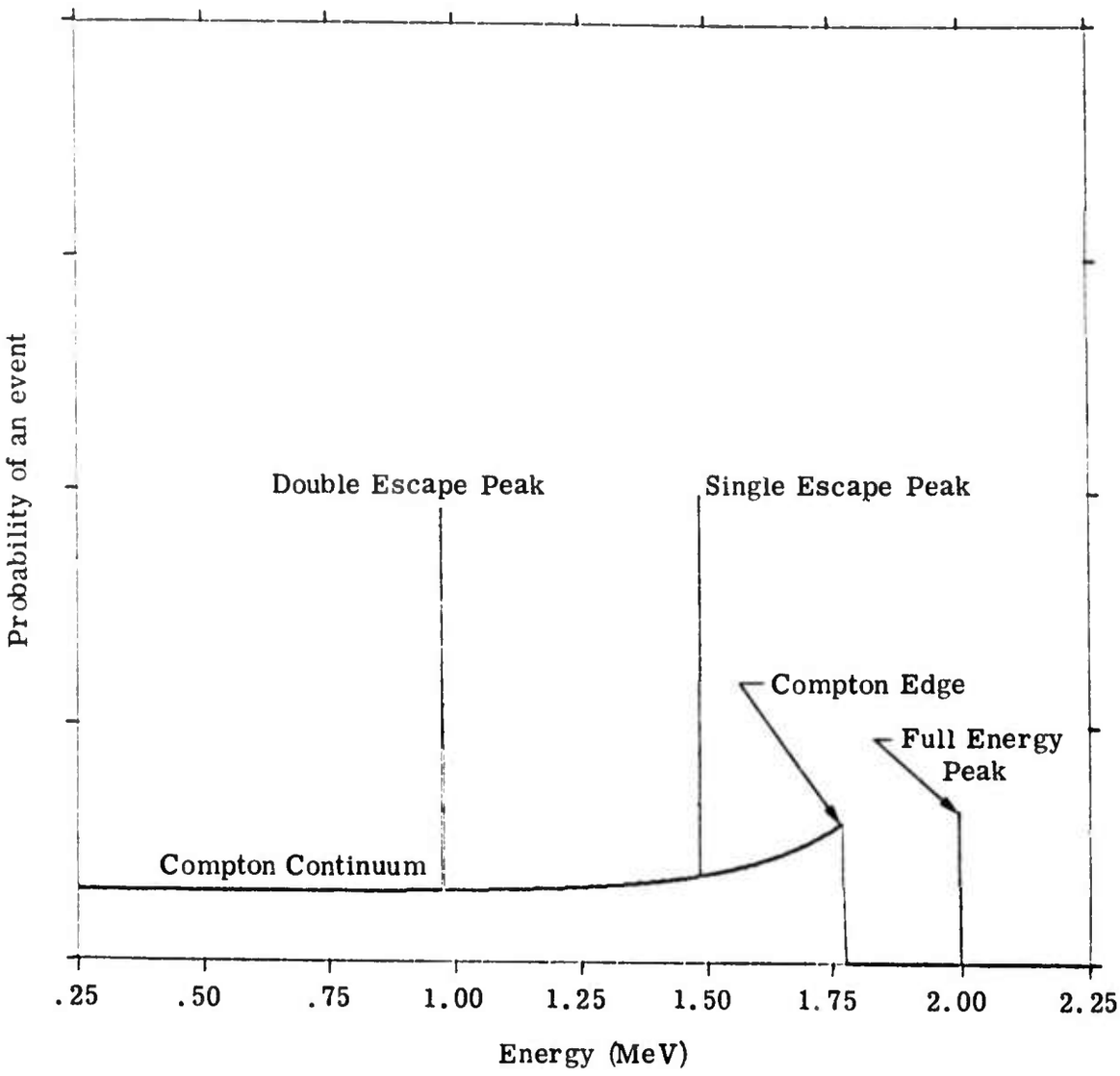

Figure 1. Ge(Li) line shape at 2 MeV.

The object of the parameterization is to minimize W with respect to β_ℓ, λ, and σ for a given energy E_o and response $A_i(E_o)$. The minimization is an iterative process. Let γ be a parameter: β_ℓ, λ or σ. Then the Taylor expansion about the n-th estimate of γ, γ^n, to determine the (n+1)-th estimate is:

$$W(\gamma^{n+1}) = W(\gamma^n) + \frac{\partial W}{\partial \gamma}\bigg|_{\gamma=\gamma^n} (\gamma^{n+1} - \gamma^n)$$

$$+ \tfrac{1}{2} \frac{\partial^2 W}{\partial \gamma^2}\bigg|_{\gamma=\gamma^n} (\gamma^{n+1} - \gamma^n)^2 \quad .$$

To minimize $W(\gamma^{n+1})$, set

$$\frac{\partial W}{\partial \gamma}\bigg|_{\gamma=\gamma^{n+1}} = 0$$

and we get

$$\frac{\partial W(\gamma^{n+1})}{\partial \gamma^{n+1}} = \frac{\partial W}{\partial \gamma}\bigg|_{\gamma=\gamma^n} + \frac{\partial^2 W}{\partial \gamma^2}\bigg|_{\gamma=\gamma^n} (\gamma^{n+1} - \gamma^n) \quad .$$

Therefore,

$$\gamma^{n+1} = \gamma^n - \frac{\partial W/\partial \gamma}{\partial^2 W/\partial \gamma^2}\bigg|_{\gamma=\gamma^n} \quad .$$

Substituting the original parameters:

$$\beta^{n+1} = \beta^{n} - \left(\frac{\partial^2 W}{\partial \beta^{n} \, \partial \beta^{n}} \right)^{-1} \frac{\partial W}{\partial \beta^{n}}$$

where the term in parentheses represents a matrix whose (ℓ, m)-th element is $(\partial^2 W)/(\partial \beta_{\ell}^{n} \partial \beta_{m}^{n})$, and $(\partial \beta^{n})$ represents the vector $(\partial W)/(\partial \beta_{\ell}^{n})$, and β represents the vector β_{ℓ} coefficients.

Also, collecting the λ and σ formulae:

$$\lambda^{n+1} = \lambda^{n} - \frac{\partial W/\partial \lambda^{n}}{\partial^2 W/\partial (\lambda^{n})^2}$$

$$\sigma^{n+1} = \sigma^{n} - \frac{\partial W/\partial \sigma^{n}}{\partial^2 W/\partial (\sigma^{n})^2} \quad ,$$

The expressions for the derivatives of W are fairly complicated and will not be presented here. Starting with a set: β_{ℓ}^{o}, λ^{o}, σ^{o}, each one is iterated in turn independently until W is minimized. This is accomplished for each E_o and it may even be possible to parameterize the resulting parameters as a function of energy.

6. EXAMPLES

Typically, an energy distribution of gamma-rays or x-rays is viewed by a spectrometer which produces a data set. This data vector or set has passed through a complex detection process and generally suffers from loss of resolution from the detection process and generally suffers from loss of resolution from the detection process and from statistical noise. It is the purpose of the MAZE program to remove degradation imposed by the detector, to minimize the effects of statistical fluctuations and to construct an image spectrum that corresponds as closely as possible to the spectrum impinging on the detector (the object spectrum).

6.1 EXAMPLE 1, SIMULATED DATA

To test the performance of the MAZE program, it is desirable to use a data set for which the object spectrum and the detector response are precisely known. This was most conveniently done by manufacturing a data set. An object spectrum composed of three delta functions on an exponential continuum, Ae^{-Bx}, was acted upon with Gaussian smearing to simulate a detector response function. The full width at half maximum, FWHM, of the Gaussian function was kept constant across the spectrum. Appropriate statistics were introduced by using a Monte Carlo type code to accumulate 750,000 counts, distributed over sixty channels, into the data spectrum.

The resulting data spectrum, Figure 2, contains a single, well resolved peak, two moderately overlapping peaks and a continuum. The correct parameters of the peaks and the exponential continuum are listed in Table 1.

TABLE 1

Peak No.	Central Channel No.	Area (Counts)	FWHM (Channels)
1	12.0	161108±401	5.7
2	36.0	161108±401	5.7
3	46.0	120831±348	5.7
Exponential Continuum $7533e^{-0.013585x}$ (x in channels)			

The spectrum was submitted to MAZE for unfolding and the resulting image spectrum is shown in Figure 3. The image spectrum closely approximates the object spectrum used to generate the data set. The enhanced peaks approach delta functions and the background is an exponential with only minor deviations. Parameters of these features are given in Table 2. The statistical fluctuations presented in the data set have been substantially reduced in the image spectrum.

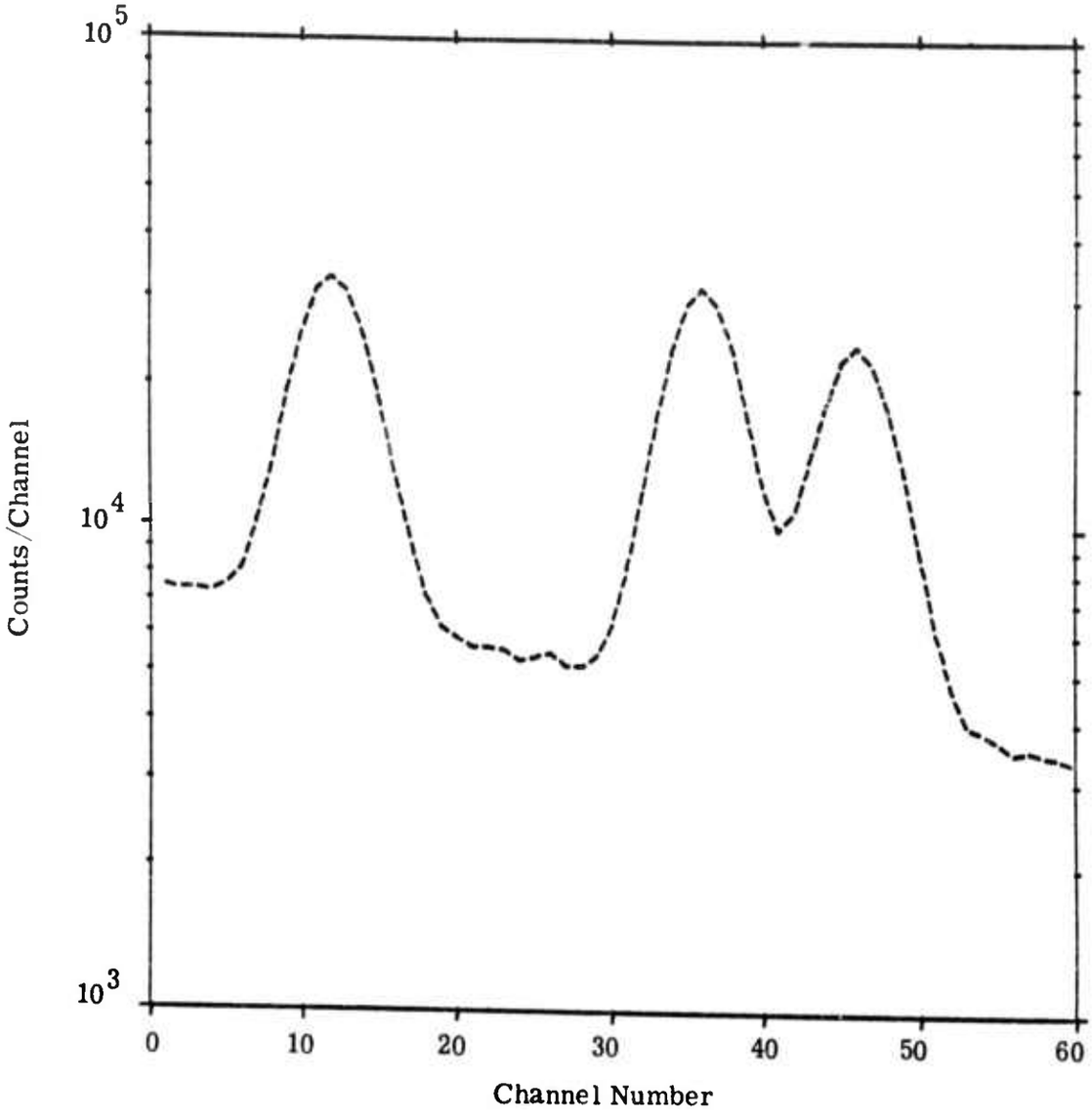

Figure 2. Simulated x-ray data.

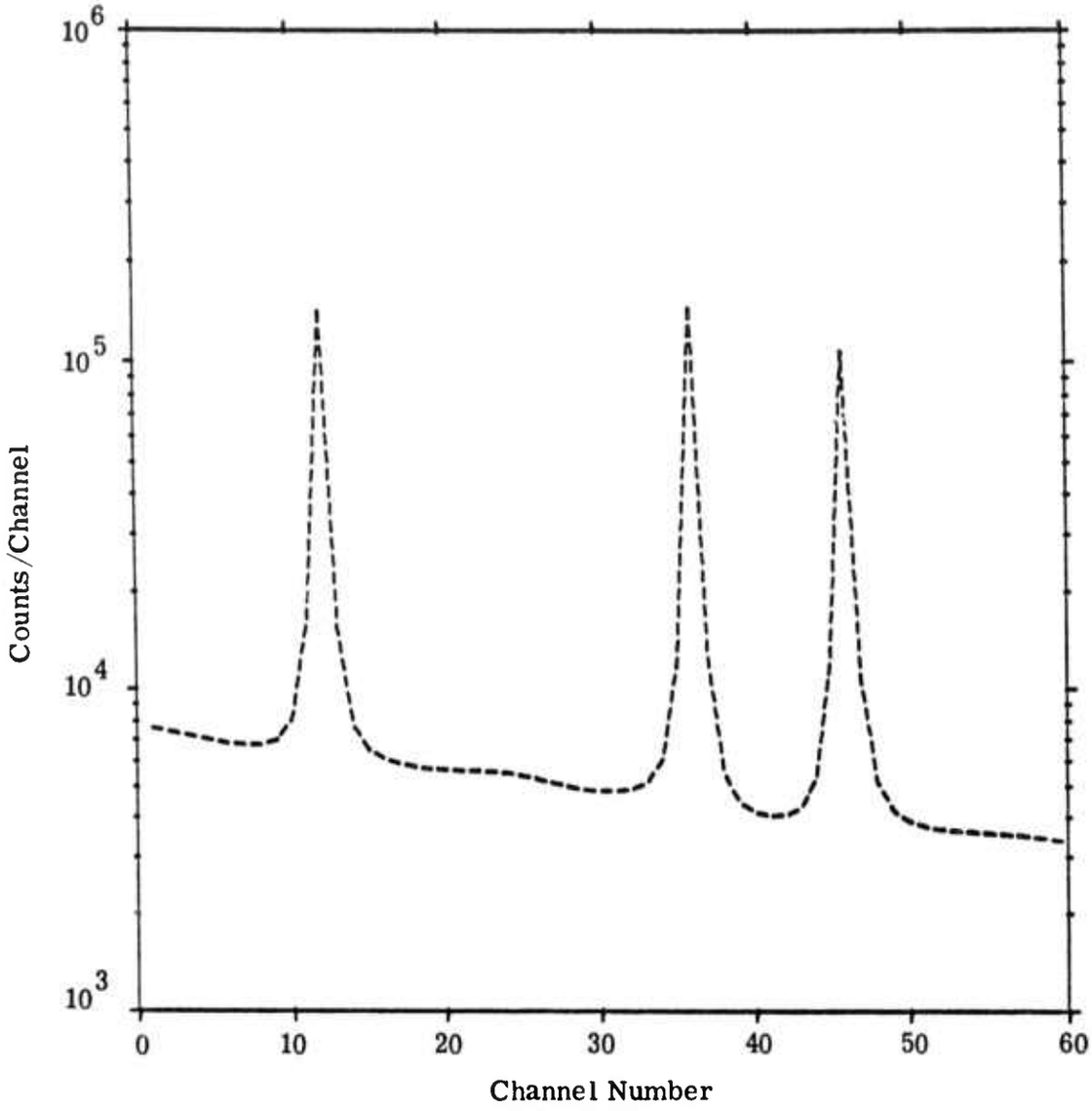

Figure 3. Image spectrum (enhanced spectrum).

TABLE 2

Peak No.	Central Channel No.	Peak Channel (Counts)	Percent of Area	Three Channels (Counts)	Percent of Area	FWHM (Channels)
1	12.0	139892	87%	158653	98+%	1.01
2	36.0	144906	90%	160566	99+%	0.97
3	46.0	103405	86%	118540	98%	1.03

Exponential Continuum $7584e^{-0.01404x}$

The application of the detector response matrix on the calculated image spectrum should, if the image spectrum is correct, reproduce the inputed data set within statistical limits. MAZE performs the calculations and obtains these statistical deviations channel by channel (Figure 4). In this example the deviations are random and indicate that the calculated image spectrum reproduces the data set quite well across the entire spectrum.

An attempt is made by MAZE during the unfolding process to distinguish between the discrete and continuum portions of the spectrum and to provide separate outputs for the discrete portion, Figure 5, and for the continuum portion, Figure 6. The separation is only partially successful. In Figure 5 the peaks are seen riding on top of a continuum that amounts to about 10 percent of the exponential background and in Figure 6 the continuum is, of course, about 10 percent low but it also has bothersome oscillations. There

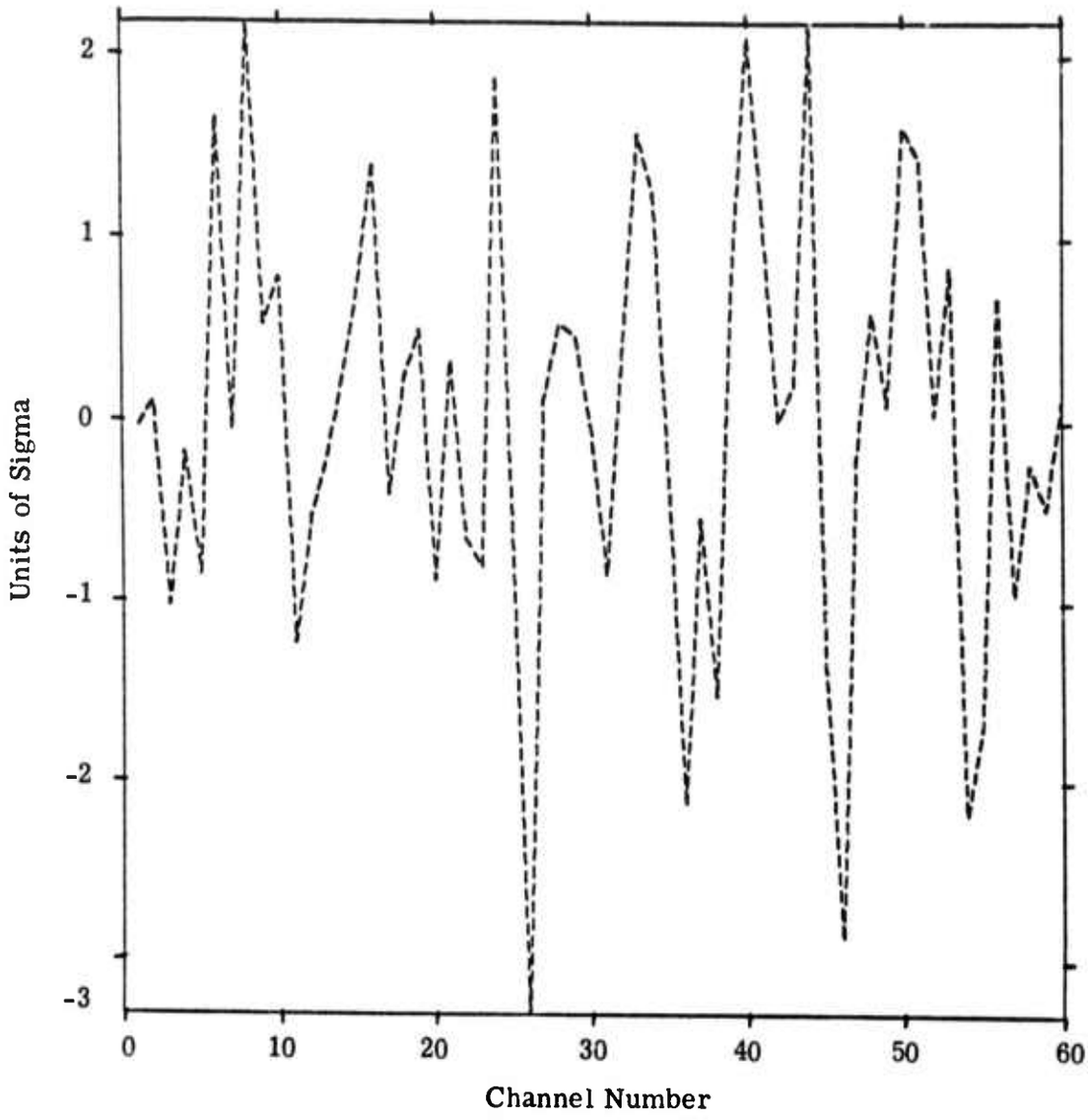

Figure 4. Deviations.

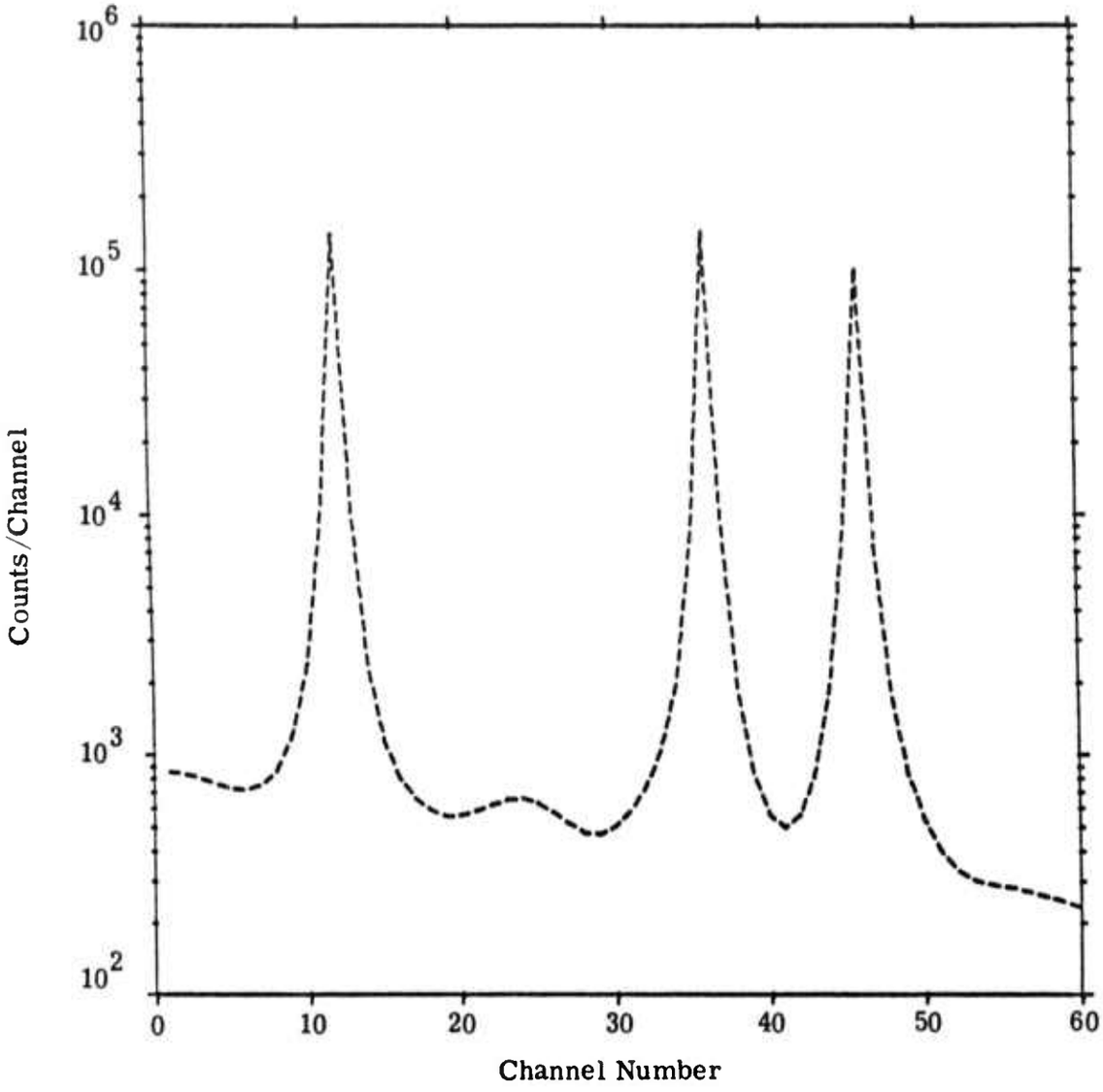

Figure 5. Discrete spectrum.

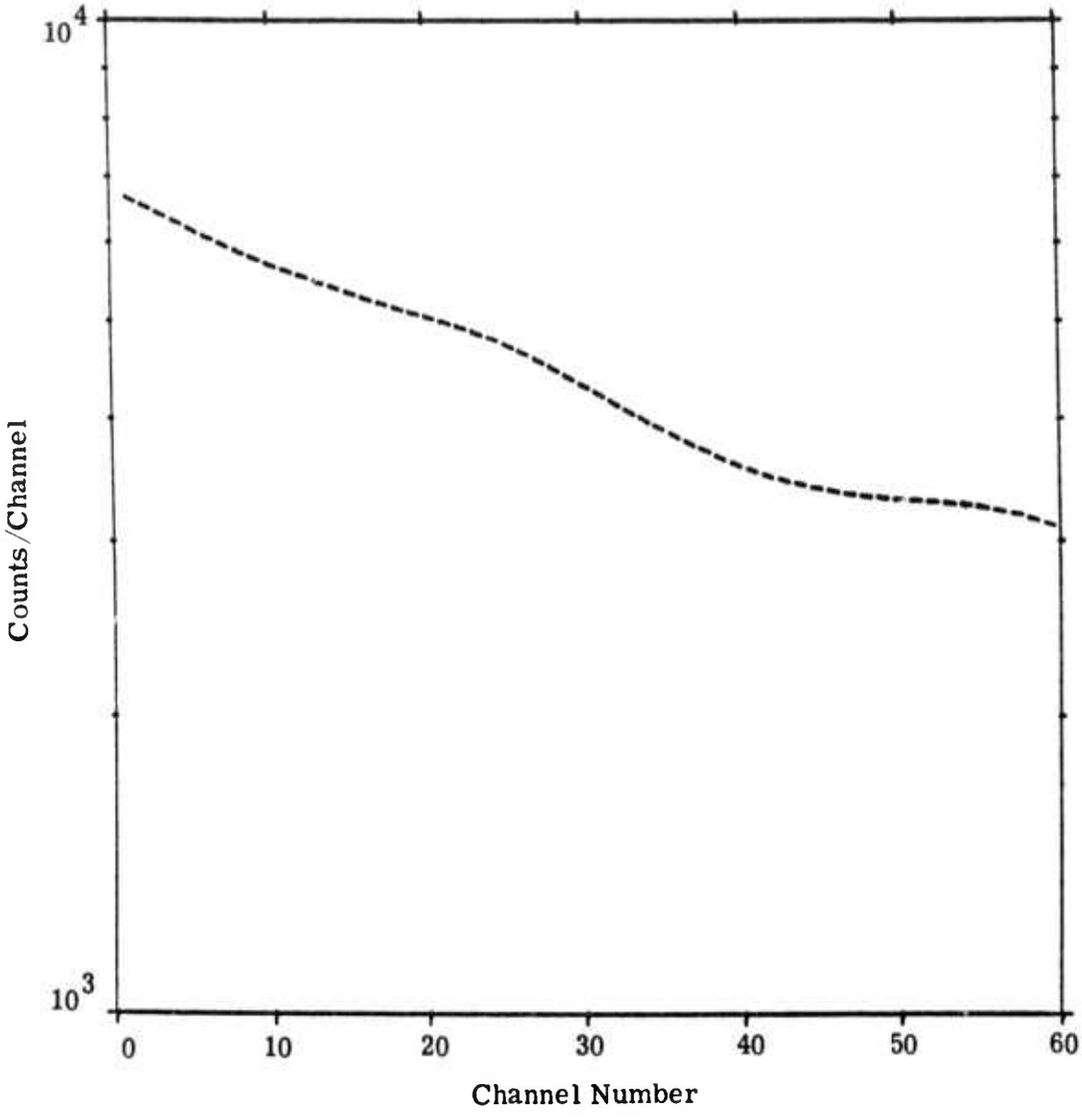

Figure 6. Continuum.

is no inherent reason that these shortcomings cannot be eliminated and, in fact, a more recent version of the code has nearly completely eliminated these effects.

6.2 EXAMPLE 2, SIMULATED DATA

A second spectrum was manufactured to provide a more exacting test of the MAZE code performance. The starting point was an object spectrum composed of five delta functions on an exponential continuum. Detector smearing and the introduction of statistics were accomplished as for example number 1 above.

The resulting data spectrum, Figure 7, contains a single well resolved peak, four highly overlapping peaks and a continuum. The parameters of the peaks and the exponential making up of the data spectrum are listed in Table 3.

TABLE 3

Peak No.	Central Channel No.	Area (Counts)	FWHM (Channels)
1	12.0	152229±390	5.7
2	31.0	15223± 123	5.7
3	36.0	152229±390	5.7
4	41.0	76114±276	5.7
5	46.0	114172±338	5.7

Exponential Continuum $7022e^{-0.013585x}$ (x in channels)

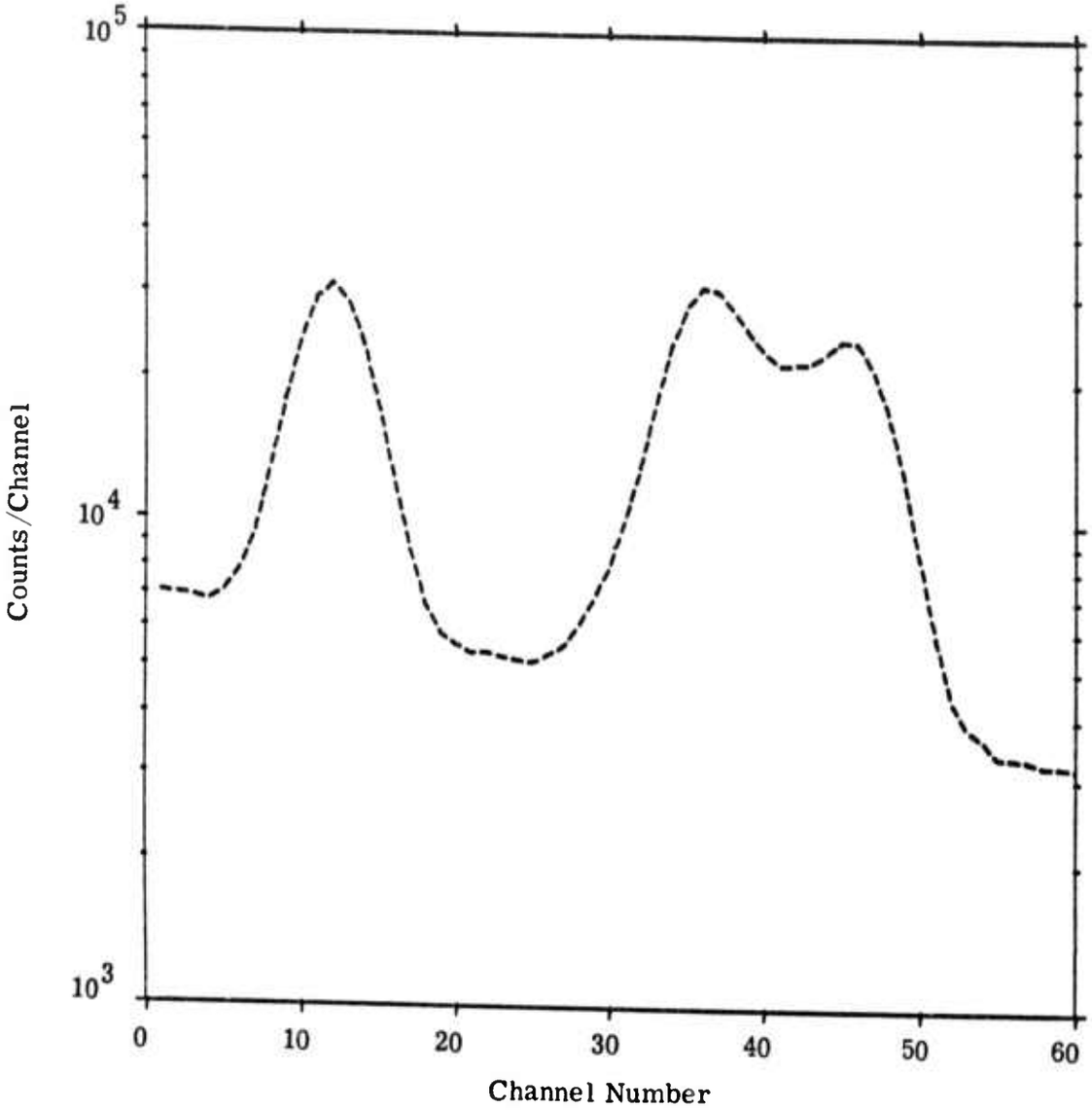

Figure 7. Simulated x-ray data.

The spectrum was submitted to MAZE for unfolding and the resulting spectrum is shown in Figure 8. The image spectrum shows considerable enhancement, the multiplet, while not resolved into four separate and distinct delta functions, is clearly made up of four peaks. Parameters of the spectral feature are given in Table 4.

TABLE 4

Peak No.	Central Channel No.	Estimated Peak Area	FWHM (Channels)	Fractional Error in Peak Area
1	12.0	151974	1.07	-0.17%
2	30.7	16677	5.61	+9.5%
3	36.0	150138	1.50	-1.4%
4	41.0	80304	3.29	+5.5%
5	46.0	112712	1.41	-1.3%

This version of MAZE tends to concentrate on the major features of the spectrum while ignoring to a large extent the minor features. A second undesirable characteristic is the tendency to add structure to the spectrum wherever there are substantial statistical fluctuations. In this example a small artificial peak was added centered at channel 20. Both of the above characteristics have been eliminated in a recent reformulation of MAZE (see Section 6.4).

6.3 EXAMPLE 3, Si(Li) X-RAY DATA

X-ray fluorescence data is an example of data which is very difficult to analyze by conventional techniques. The energy resolution

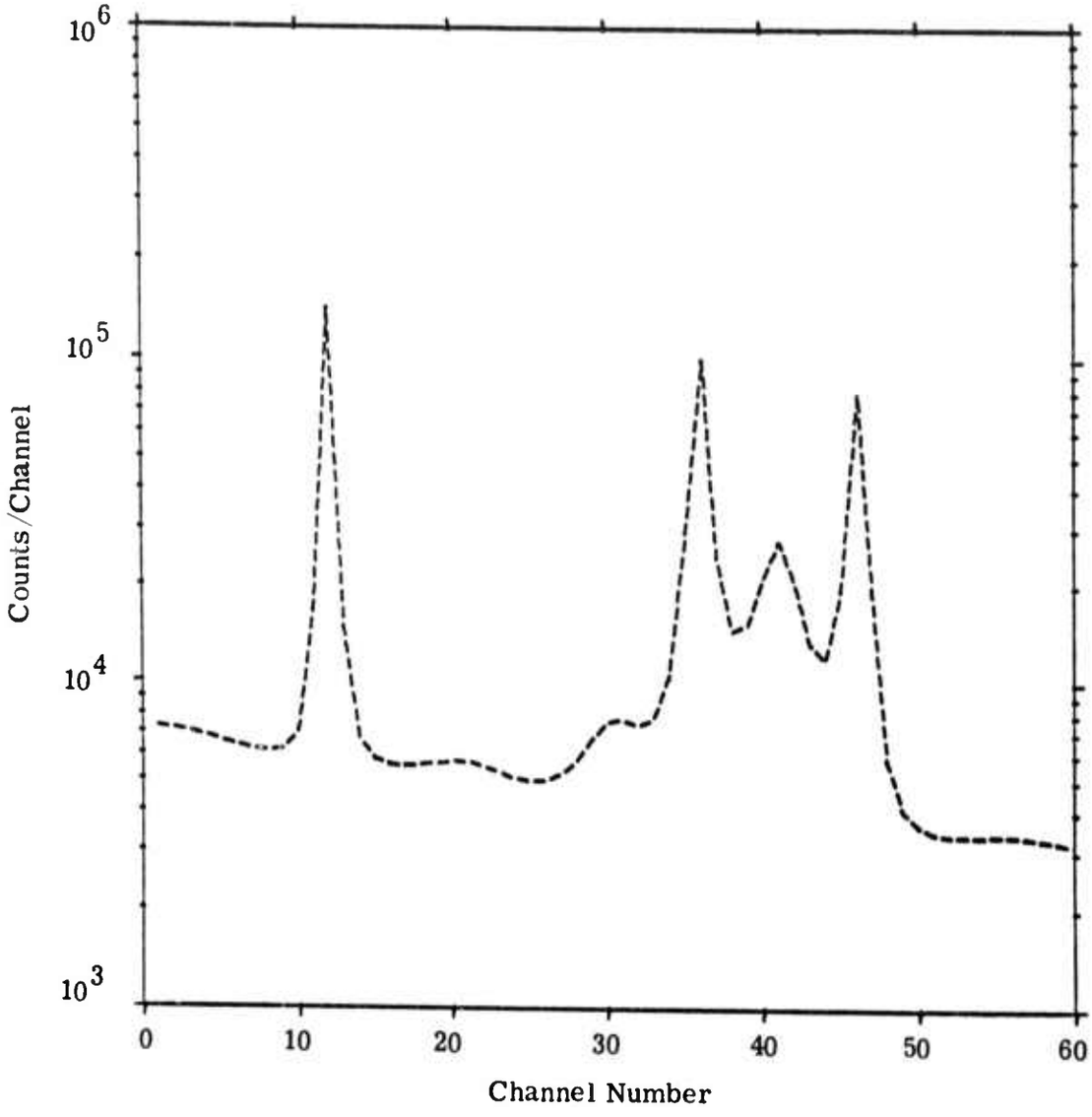

Figure 8. Image spectrum (enhanced spectrum).

afforded by state-of-the-art detectors is not sufficient to always resolve the many X-ray lines often produced in the irradiation of materials. An example of such data is shown in Figure 9. In this example there are at least ten Gaussian shaped peaks superimposed on a Bremsstrahlung continuum. Because of the overlapping nature of the peaks, the shape and intensity of the continuum is not clear. However, this information is vital in determining the area of intensity of each of the discrete lines.

The result of applying the spectral enhancement capabilities of MAZE are shown in Figure 10. Peaks 1 through 7 become clearly resolved lines and a small peak is indicated just above peak 7. In addition to confirming the suspicion that peak 9 was a doublet, MAZE suggests that peak 8 is also complex. A reasonable Bremsstrahlung continuum (see Figure 10) can be deduced from the image spectrum for use in determining line intensities. The effective energy resolution (FWHM) of the prominent peaks in the image spectrum is of the order of 41 eV (1.46 channels) as compared to 170 eV (6.0 channels) in the data spectrum.

6.4 EXAMPLE 4, Ge(Li) GAMMA RAY DATA

The statistics in the previous example were excellent, each of several of the peaks in the data spectrum contained hundreds of thousands of counts. We are not always so fortunate, often we must analyze data having poor statistics. An example of such a spectrum is shown in Figure 11. This data was taken with a Ge(Li) gamma-ray spectrometer and was obtained from W. L. Imhof of the Lockheed

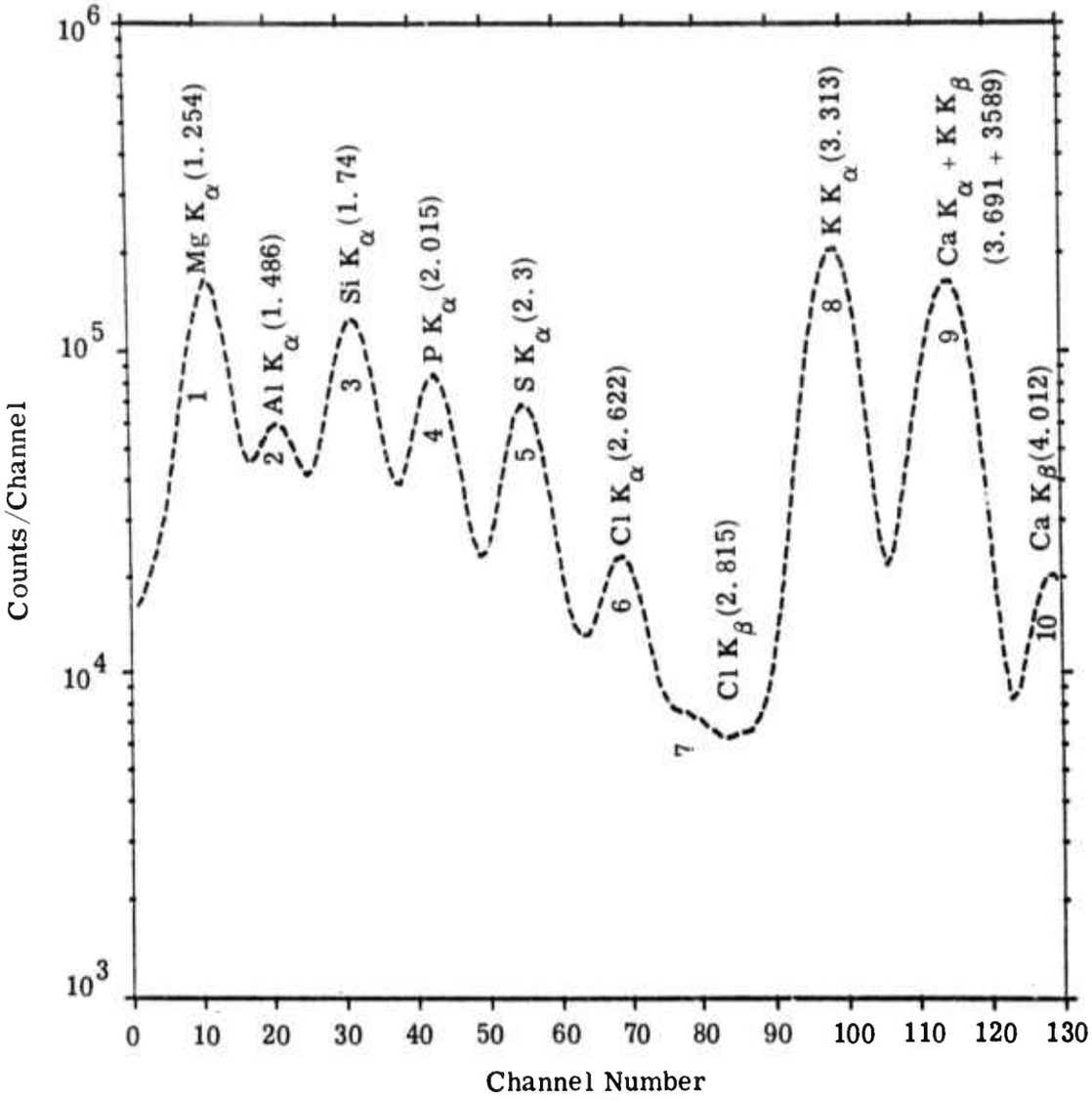

Figure 9. X-ray fluorescence data.

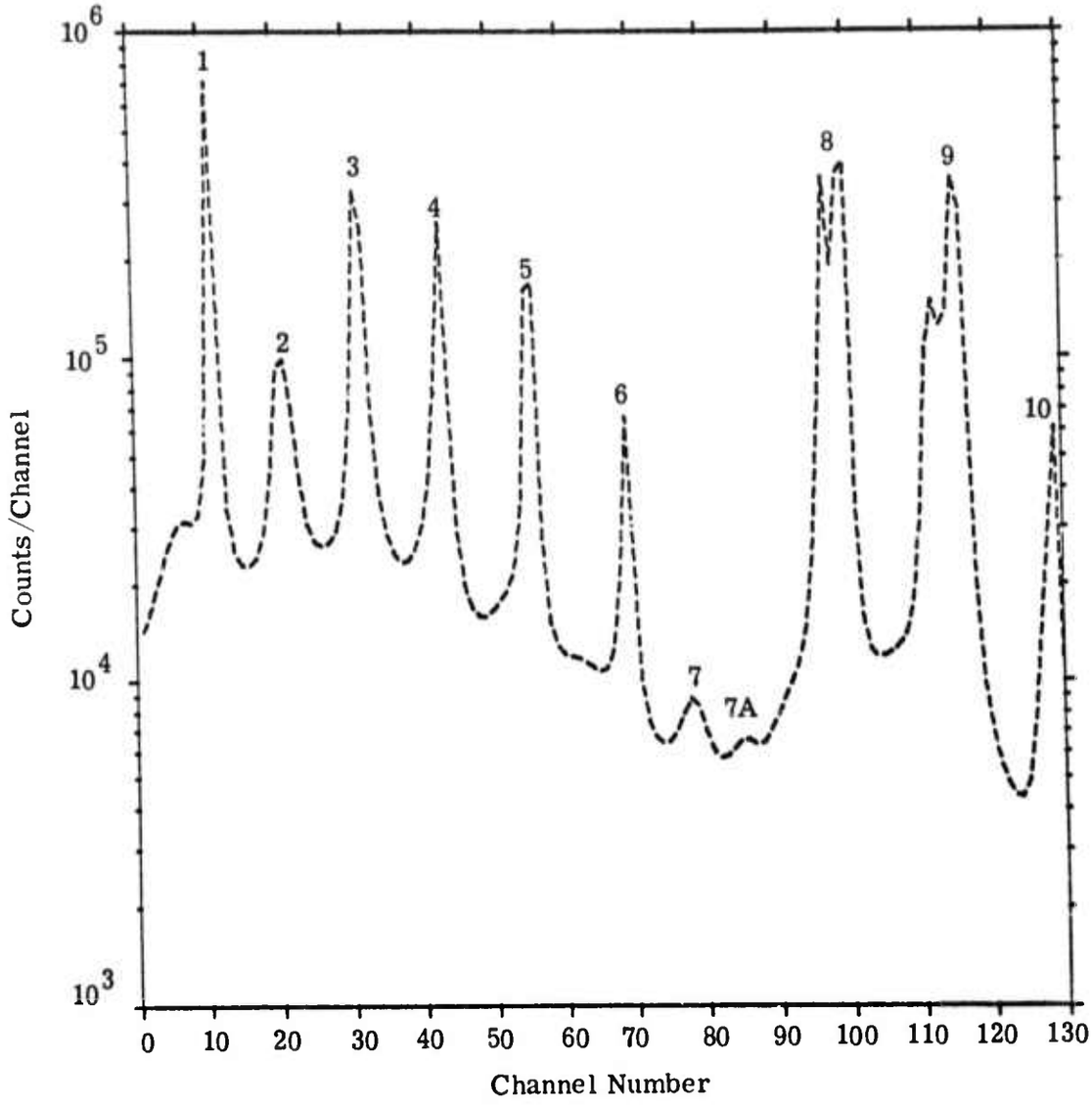

Figure 10. Enhanced x-ray fluorescence spectrum.

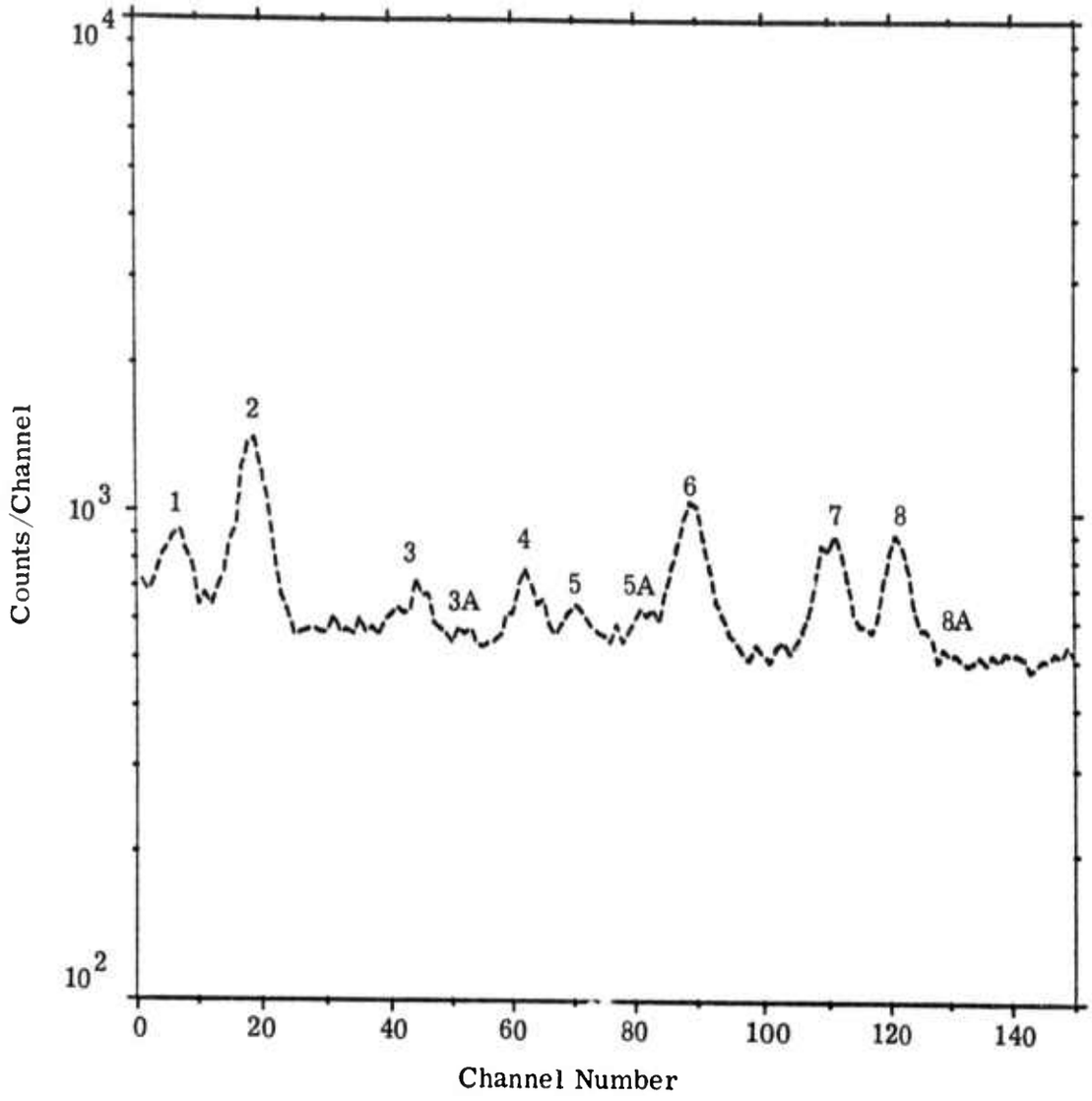

Figure 11. Ge(Li) gamma-ray data.

Space Sciences Laboratory. A visual examination of Figure 11 suggests that peaks 1 through 8 are real lines while peaks 3A, 5A, and 8A may only be statistical fluctuations.

In applying MAZE to this data it was assumed, as it was in the previous examples, that the detector response was pure Gaussian in nature. The resulting image spectrum is shown in Figure 12. The energy resolution was enhanced considerably but unfortunately the code also enhanced and amplified the statistical fluctuations thereby introducing many spurious peaks. Therefore, we must conclude that this version of MAZE is limited to applications involving data with good statistics.

Previously it was stated that a recently improved version of MAZE has been developed that handled statistical fluctuations in a more reasonable manner. The improved MAZE code was applied to the identical Figure 11 data set. The resulting image spectrum is shown in Figure 12. Not only is the energy resolution substantially enhanced but the statistical noise is greatly suppressed. All spurious peaks are eliminated. The only questionable peak that remains in the image spectrum is 5A.

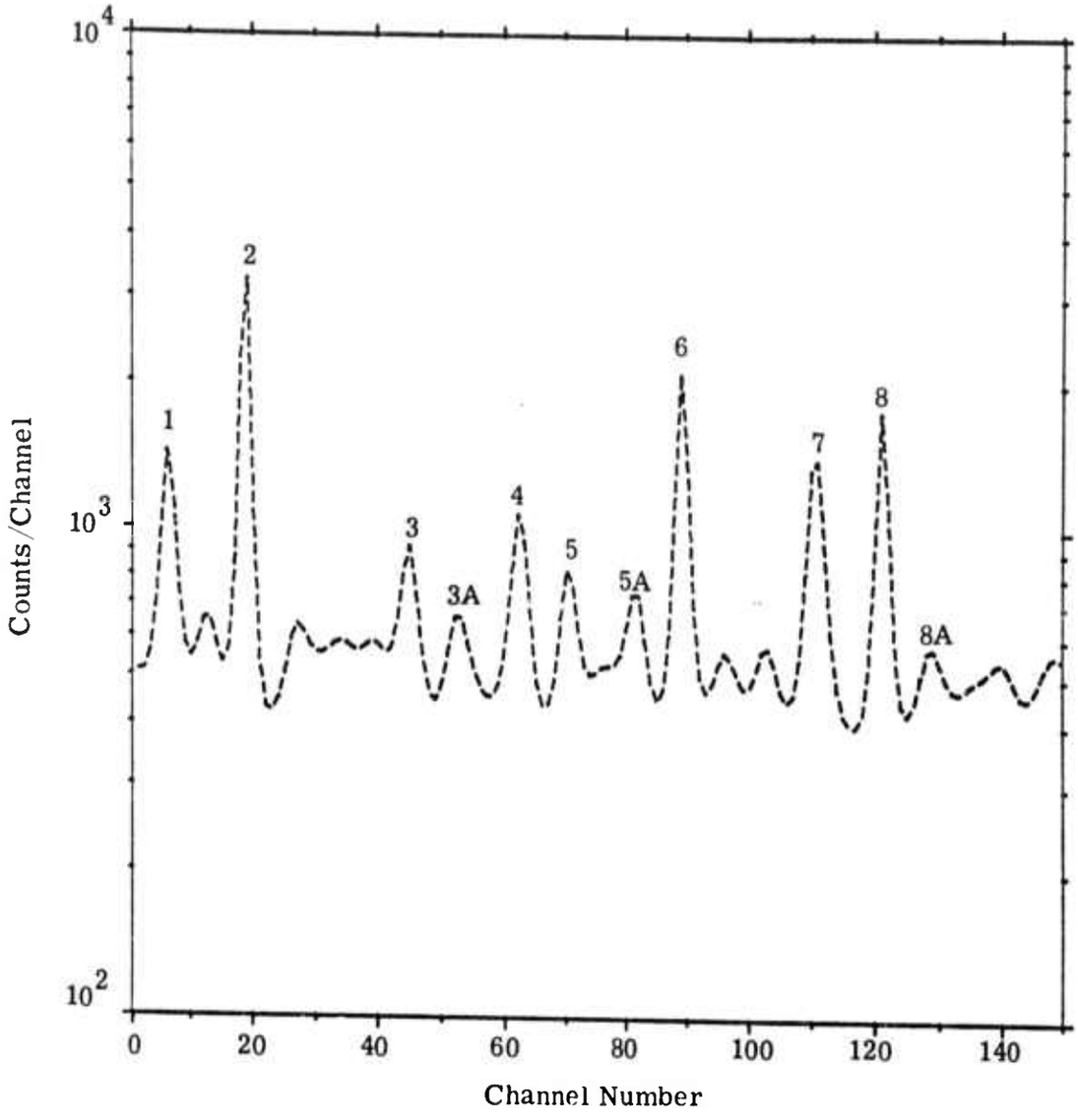

Figure 12. Enhanced gamma-ray spectrum.

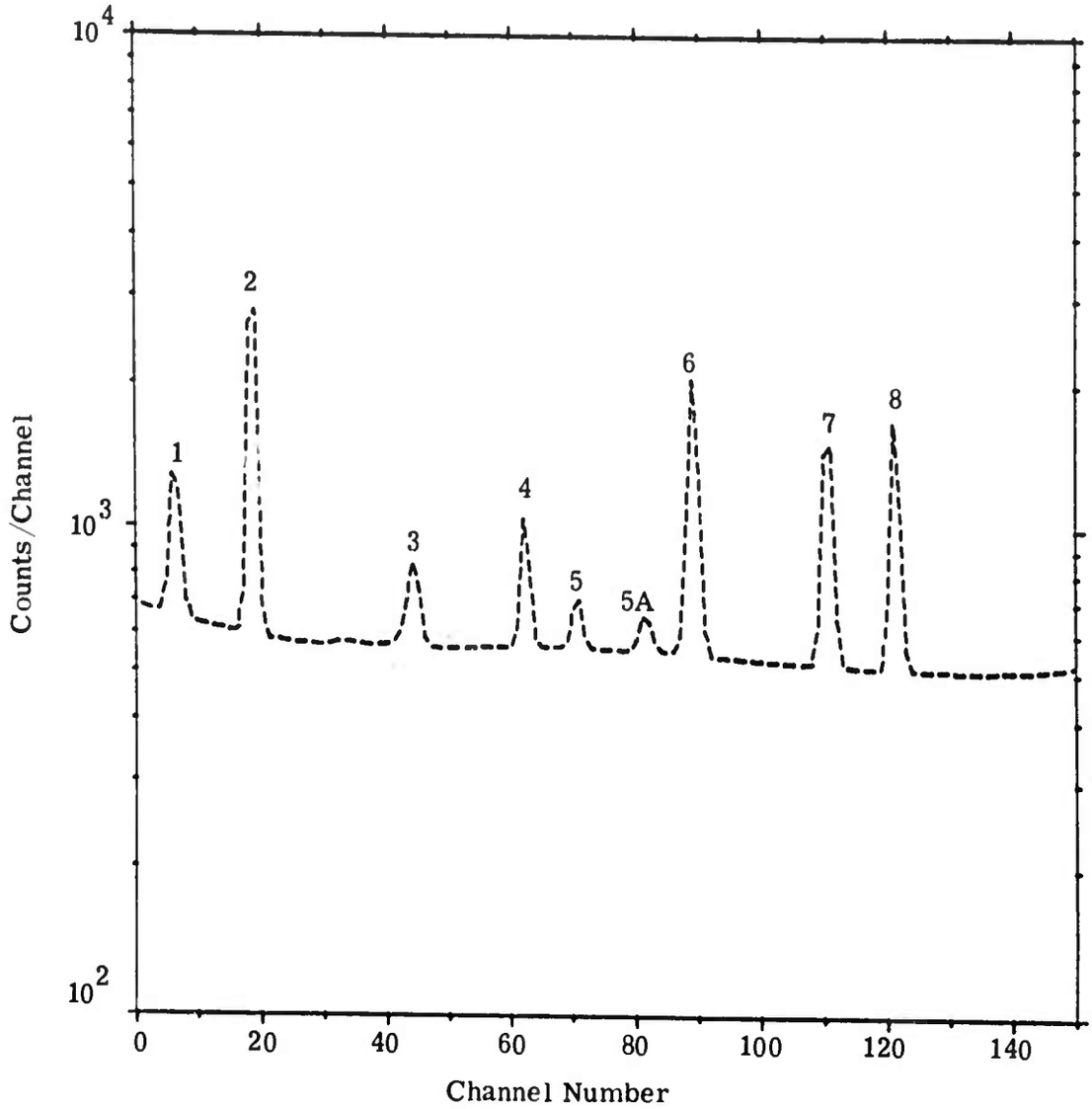

Figure 13. Improved enhanced gamma-ray spectrum.

7. CONCLUSION

The program for Illiac IV has been written in Glypnir [5] and arrangements are currently being made to run MAZE on I4. This has been delayed purposely so that the I4 system being tried is as up-to-date as possible. Consequently, there are no run-time comparisons that can be quoted; however, as previously stated, serial computers can only tackle relatively small (150-200 channels) problems because of memory limitations. The memory of I4 is also limited, nonetheless because of the improved representation of the response matrix it may be possible to run a problem with 256 channels on I4 that is core contained. For higher number of channels the matrix will be sectioned and buffered in and out of PE memory.

The response matrix is assumed to be nearly diagonal (see Section 5) and only the first 64 non-zero values of each row are kept. This allows the inclusion of structure into the matrix that is not strictly Gaussian. It also allows change of resolution as a function of energy.

There is an index associated with each row which indicates the column number of the first non-zero element. Each PE contains one element of the row and thus a whole row is available for computation. Experience indicates that 64 is a high enough number of non-zero elements to keep in the response matrix for most foreseeable applications. That number was obviously selected because of the nature of I4.

REFERENCES

1. S. M. Sperling and H. Kendrick, "Numerical and Experimental Studies of Spectral Unfolding", Gulf Radiation Technology, Gulf-TR-10486, May 1971.

2. Martin Sperling, "Spectral Unfolding: It's Mathematical Basis, Implementation and Application with MAZE2", SAI-73-574-LJ, DNA 2990F, October 1972.

3. Burroughs Corporation, "ILLIAC IV Systems Characteristics and Programming Manual", Defense, Space and Special Systems Group of Burroughs Corporation, Report No. 66000D, IL4-PM1, June 1, 1972.

4. S. A. Denenberg, "An Introductory Description of the ILLIAC IV System", Volume 1, ILLIAC IV Document No. 225, Department of Computer Science, University of Illinois, July 15, 1971.

5. T. Layman and D. Baer, "GLYPNIR Reference Manual", ILLIAC Project Document, Computer Center of the University of California, San Diego, September 1972.